Cerebral Cortex (2019.3) :.

Premotor Cortex Provides a Substrate for the Temporal Transformation of Information During the Planning of Gait Modifications.

Toshi Nakajima, Nicolas Fortier-Lebel, Trevor Drew

Premotor cortex provides a substrate for the temporal transformation of information during the planning of gait modifications

By

Toshi Nakajima[1], Nicolas Fortier-Lebel[2,3] and Trevor Drew[2,3]

[1]The Research Center for Brain Function and Medical Engineering
Asahikawa Medical University 2-1, 1-1,
Midorigaoka-Higashi,
Asahikawa 078-8510,
Japan
Tel: +81-166-68-2884

[2]Département de Neurosciences,
[3] Groupe de recherche sur le système nerveux central (GRSNC),
Université de Montréal,
Pavillon Paul-G. Desmarais,
C.P. 6128, Succursale Centre-ville,
Montréal, Québec, H3C 3J7
Canada

Running Title: Activity in premotor cortex during locomotion

Correspondence: Dr. Trevor Drew[2]
Tel: (514) 343 7061
Email: Trevor.Drew@umontreal.ca

Major Subject Area: Neuroscience

Total figures: 17
Text figures: 15
Supplementary Figures: 2
Black and white figures: 2
Color figures: 15
Tables: 2
Abstract: 148 words

Abstract

We tested the hypothesis that the premotor cortex (PMC) in the cat contributes to the planning and execution of visually-guided gait modifications. We analyzed single unit activity from 136 cells localized within layer V of cytoarchitectonic areas 6iffu and that part of 4δ within the ventral bank of the cruciate sulcus while cats walked on a treadmill and stepped over an obstacle that advanced towards them. We found a rich variety of discharge patterns, ranging from limb-independent cells that discharged several steps in front of the obstacle to step-related cells that discharged either during steps over the obstacle or in the steps leading up to that step. We propose that this population of task-related cells within this region of the PMC contributes to the temporal evolution of a planning process that transforms global information of the presence of an obstacle into the precise spatio-temporal limb adjustment required to negotiate that obstacle.

Keywords: Locomotion, cat, visually-guided gait modification, single neuron recording, voluntary movement.

Or the right limb

Introduction

The ability to make anticipatory modifications of gait based on visual information is essential to our capacity to walk on uneven or cluttered terrain. While the timing and pattern of the basic, rhythmic, coordinated locomotor pattern largely depends on spinal neuronal networks (Grillner S and P Wallen 1985; Rossignol S 1996), previous studies on cats have shown that the primary motor cortex (MI) is essential for the precise execution of gait modifications (Beloozerova IN and MG Sirota 1993; Drew T 1993; Friel KM et al. 2007; for review Drew T et al. 2008). Subsequent studies have further highlighted the importance of the posterior parietal cortex (PPC) in planning gait modifications based on visual input (Beloozerova IN and MG Sirota 2003; Lajoie K and T Drew 2007; McVea DA et al. 2009; Andujar J-E et al. 2010; Marigold DS et al. 2011; Drew T and DS Marigold 2015; Wong C et al. 2017) and particularly in determining the relative location of an obstacle with respect to the body (Marigold DM and T Drew 2017). Indeed, it is probable that impairment of the ability to accurately localize an object leads to the errors in the capacity to successfully negotiate an obstacle that ensue following damage to the PPC (Lajoie K and T Drew 2007).

While object localization and the production of the motor activity that results in the step over an obstacle are critical aspects in planning and executing gait modifications, they represent only the starting and finishing stages of a complex planning process (Marigold DS *et al.* 2011; Drew T and DS Marigold 2015). In the task used in this laboratory, in which cats are trained to walk on a treadmill and to step over an obstacle that advances towards them, these include: determining obstacle attributes; selecting which limb will be the first to step over the obstacle; adjusting the gait as the obstacle advances towards the cat so as to allow the other limb to be appropriately placed in front of the obstacle (the plant limb); and adjusting the parameters of the limb trajectory on the basis of the obstacle attributes (size and shape) (Fig. 1A). Some of these processes are probably planned sequentially while others occur in parallel. We propose that each of these processes results from the recruitment of populations of neurons with activity patterns that are generally consistent with those illustrated in Fig. 1C. While neuronal populations contributing to these functions might be distributed within a large network of cortical and subcortical structures, the critical contribution that the premotor cortex (PMC, area 6) makes to planning voluntary movements in primates (see below) makes it a prime candidate for regulating at least some of these planning stages.

In primates, for example, arm movements are impaired by both ablation (Moll L and HG Kuypers 1977; Brinkman C 1984) and by pharmacological inactivation (Kurata K and DS Hoffman 1994; Shima K and J Tanji 1998; Fogassi L et al. 2001) of the PMC, particularly when the movement has to take into account the context of the activity. Complementary studies using single-unit recording (Wise SP and KH Mauritz 1985; Rizzolatti G et al. 1990; Crammond DJ and JF Kalaska 2000; Hoshi E and J Tanji 2000; Shima K and J Tanji 2000; Kakei S et al. 2001; Cisek P and JF Kalaska 2005) have further shown correlates between cell discharge and different parts of the planning and execution of discrete voluntary movements, while microstimulation of area 6 has

shown that complex movements can be evoked by prolonged trains of stimulation applied to this area (Graziano M 2006). In addition, several regions of the PMC have direct projections to MI (Muakassa KF and PL Strick 1979; Luppino G et al. 1993; Tokuno H and J Tanji 1993; Dum RP and PL Strick 2002), which would allow them to directly affect motor activity.

Although studies in humans using non-invasive methods (Fukuyama H et al. 1997; Hanakawa T et al. 1999; Malouin F et al. 2003; Shine JM et al. 2013; Wagner J et al. 2014; Sacheli LM et al. 2018) suggest a similar contribution of higher motor areas to planning locomotion, there are very few studies in animals that examine, at the single cell level, the contribution of non-primary motor areas to locomotion (see, however Foster JD et al. 2014) and none that have specifically addressed the contribution of the higher motor areas to the planning of gait modifications during locomotion.

In cats, Hassler and Muhs-Clement (Hassler R and K Muhs-Clement 1964, see also Ghosh S 1997b) identified several cytoarchitectonic divisions of area 6 (generally assumed to correspond to non-primary, premotor cortex) in the agranular cortex of the frontal portion of the cerebrum, both anterior to and within the cruciate sulcus. These divisions include areas 6aα, 6aβ, 6aγ and 6iffu and are identified on a flattened diagram of the frontal cortex in Fig. 3 (see also Fig. 12). In addition, Hassler and Muhs-Clement also identified several-subdivisions of area 4. In addition to the primary motor cortex (M1, area 4γ), these include non-primary areas 4δ, 4sfu and 4fu (see Fig 3). Some of the subregions in area 6 and non-primary regions of area 4 have direct connections to M1 (Ghosh S 1997a, 1997d; Andujar J-E and T Drew 2007) as well as to the pontomedullary reticular formation (Berrevoets CE and HGJM Kuypers 1975; Matsuyama K and T Drew 1997; Rho M-J et al. 1997) and some of these regions, including the non-primary motor regions of area 4, have been putatively identified as being analogous to the primate's PMC (Hassler R and K Muhs-Clement 1964; Avendaño C et al. 1992; Ghosh S 1997d). Although it is tempting to postulate that these divisions are, indeed, analogous to the premotor areas of primates (Ghosh S 1997d; Nakajima T et al. 2015) and that they are involved in planning motor activity, as in primates, there have been no systematic studies of the characteristics of cells in cat PMC during voluntary movements, including locomotion. Such studies are essential to determine whether cells in these different cytoarchitectonic regions discharge in a manner consistent with a contribution to planning movement.

In the context of our interest in the neural mechanisms involved in locomotor control, we tested the hypothesis that neurons within sub-divisions of area 6 and the non-primary regions of area 4 (together referred to here in general terms as PMC) contribute to the planning of visually-guided gait modifications. To test this hypothesis, we recorded the activity of single neurons in selected divisions of the PMC of cats performing our behavioral task in which they walk on a treadmill and modify their gait to step over an obstacle that advances toward them (Drew T 1988, 1993; Andujar J-E *et al.* 2010). The present report focuses on cells located in the deeper portions of the ventral bank of the cruciate sulcus (areas 6iffu, 4fu and 4δ) because we found evidence of cells showing task-related activity prior to the step over the obstacle in this region in a preliminary study (Nakajima et al. 2015). In addition, we compare our results from the current recordings with those from previous recordings in the posterior parietal cortex (PPC) to determine the degree of similarity and difference in the discharge characteristics of neurons in the two areas.

Our results show the presence of several categories of neurons that discharge at different times prior to, and during, the step over the obstacle. We propose that the pattern of discharge in these different categories of neurons represents different aspects of the planning process and the subsequent step over the obstacle, consistent with several of the hypothetical planning steps illustrated in Fig. 1. These include: cells discharging in advance of the step over the obstacle that we propose are implicated in obstacle localization and possibly limb selection; as well as other cells discharging in relationship to the placement of the limb contralateral to the recording site in front of the obstacle in advance of the step over the obstacle by the other limb. We propose that yet other cells contribute to the coordination of the fore- and the hindlimbs as they step, in turn, over the obstacle. We discuss the possibility that the regions in the cat premotor cortex from which these cells were recorded are analogous to primate areas pre-SMA (area 6iffu) and SMA (area 4δ) and that these regions in the cat perform similar functions to those in the analogous regions of the primate PMC.

Materials and Methods

Training and Surgery. Data were obtained from two male adult cats (P1 and P2, weight 4-5 kg) which were initially trained to walk for periods of ~ 10 min on a treadmill at a speed of $0.45 m \cdot s^{-1}$ and then to step over two obstacles attached equidistantly (spacing 3m) to a second belt moving at the same speed as the treadmill. The cats normally took 12-14 steps between the obstacles which were visible to the cat for 10-12 steps before the step over the obstacle. For cat P1, each obstacle had a 5 cm x 5 cm square cross section. For cat P2, both obstacles had a round cross section with different diameters (5 cm and 10 cm). These obstacles spanned the entire width of the treadmill.

Following training, the cats were prepared for aseptic surgery under general anesthesia. They were premedicated with a mixture of acepromazine maleate (50 μg/kg), glycopyrrolate (10 μg/kg), and ketamine (11 mg/kg) and were then intubated and anesthetized with isoflurane (2-3 % with oxygen). Fluids, as well as corticosteroids (methylprednisolone, Solu-medrol, 15-30 mg/kg) to prevent cortical edema, were administered through a catheter. Antibiotics (8 mg/kg, cefovecin sodium) were injected subcutaneously. Heart rate, body temperature and blood oxygen saturation were continuously monitored. The animals were placed in a stereotaxic frame using a pair of atraumatic ear bars coated with xylocaine; petroleum jelly was applied to the eyes to prevent desiccation of the cornea. A craniotomy was performed over the right hemisphere to expose the pericruciate cortex and the ansate sulcus. A recording chamber (internal dimensions, 10 × 15 mm) was placed over the cranial aperture tilted rostrally at a 25° angle with respect to the stereotaxic horizontal plane and fixed in place with dental acrylic (Drew, 1993). To identify corticofugal neurons in layer V of the cortex, in one cat (P1), two arrays of microwires were stereotaxically implanted into the cerebral peduncle (A 4.0, L 3.0 and A 4.0, L 5.0) by using a harpoon assembly (Palmer CI 1978; Drew T 1993). For the other cat (P2), one array was implanted into the cerebral peduncle (A 4.0, L 3.5) and the other one into the pyramidal tract (P 7.0, L 1.2). Pairs of Teflon-coated, braided stainless steel wires were implanted into selected muscles of the forelimbs, hindlimbs, and neck (Drew T et al. 1986; Drew T 1993). Analgesics (buprenorphine, 5μg/kg) were administered for 3-4 days postoperatively. The cats were allowed to recover for 1-2 weeks before beginning experiments. All surgical procedures followed the recommendations of the Canadian Council for the Protection of Animals and protocols were approved by the local animal ethics committee.

Protocol. During each experimental session, a custom-made microdrive was attached to the recording chamber and a glass-insulated, tungsten microelectrode (impedance of 0.5-1.5 MOhm) was advanced into the cortex at an angle perpendicular to the recording chamber. We identified cortical layer V by the presence of neurons discharging antidromically in response to stimulation of the microwires implanted in the cerebral peduncle or the pyramidal tract. Neurons that discharged at constant latency to the stimulation and that satisfied the criteria of the collision test (Lipski J 1981) were classified as corticofugal neurons or pyramidal tract neurons (PTNs).

Neuronal activity was recorded for a period of 2-10 min during which the cat walked on the treadmill and stepped over the obstacles. When possible, each neuron was subsequently tested to determine a receptive field. Initially, we explored the entire body, as far as possible, to determine whether cells responded to light touch of the fur or skin. Such cells were classified as cutaneous. When a cutaneous receptive field was not detectable, we passively manipulated the limb to determine if we could activate the neuron in response to proprioceptive input. We also tested each

neuron for visual responses by moving an object in front of the cat. We paid particular attention to whether the neuron discharged to a looming stimulus by moving the object toward the cat. At the end of the recording session (1-2 hrs), intracortical microstimulation (ICMS; cathodal current, 11 pulses at 330 Hz, duration 0.2 ms, 5-100 μA) was applied through the electrode at the location of the last recorded neuron in layer V. To aid in histological reconstruction, small electrolytic lesions (cathodal current, single pulse at 50 μA, duration 10 s) were made in selected penetrations.

Electromyographic (EMG) activity was amplified, filtered (100 - 450 Hz), and then sampled at a frequency of 1 kHz. Unit activity was sampled at 100 kHz. DVD recordings were made of all experiments and synchronized to the EMG and unit data by recording a digital time code on both the DVD and the digitized data file. This allowed us to inspect the recordings off-line to ensure that only periods of stable walking were included for analysis.

Data analysis.

*Identification of steps***.** The data were first displayed on a computer screen and stable sequences of locomotion selected for further analysis. A custom program was used to mark the onset and offset of the locomotor activity of selected muscles as well as to identify selected series of step cycles during the voluntary gait modification. The time of initiation of each step cycle was defined with respect to the onset of the EMG activity of a forelimb flexor muscle, either cleidobrachialis (ClB) or brachialis (Br). For each sequence of locomotion, we identified whether the left limb (contralateral to the recording hemisphere) or the right limb was the first to step over the obstacle. We refer to these as left and right limb lead conditions, as in Marigold and Drew (2017). These correspond, respectively, to lead and trail conditions with respect to the contralateral (left) limb, which we used in previous publications (Drew 1993; Andujar et al. 2010). In addition, we separately identified steps over the smaller and larger of the two obstacles for cat P2. As a reference, we identified the 4^{th} step cycle before the lead step as a *control step* (unobstructed locomotion) as this step occurred before any change in EMG or neuronal discharge activity was observed during the task (see also Andujar J-E *et al.* 2010 and Drew T 1993).

Neuronal discrimination and data selection. Neurons were selected for analysis if off-line inspection showed that action potentials were well isolated throughout the recording period and if we recorded ≥ 4 steps over each obstacle in both left and right lead conditions. In cat P2, we analyzed only cells that had ≥ 4steps over each of the 2 different obstacles in each condition to allow us to analyze the effect of obstacle size on cell discharge (see below). Requiring 4 steps over each obstacle in cat P2 removed only 9 cells from our final database compared to a criterion in which we accepted 4 steps over either obstacle. Single-unit activity was isolated by using an off-line spike sorter (Plexon, TX). Recorded data were then processed as described in previous publications from our laboratory (Drew T 1993; Lavoie S and T Drew 2002; Andujar J-E *et al.* 2010).

*Normalizing and averaging of EMG and neuronal activity***.** Neuronal firing activity during each trial was converted into instantaneous frequency (1000/inter-spike interval) and EMG activity was rectified. Data in the individual trials were then filtered at 25 Hz. Signals in each trial were next aligned and normalized with respect to the onset of activity in the flexor muscle used to synchronize the data. Both EMG and neuronal activity were normalized by resampling the activity into 512 equal bins by using the method described by Udo et al. (1982); binwidth = average cycle duration/512: ~2ms). Data in each bin were then averaged for 3 step cycles before the step over

the obstacle and for 1 or 2 step cycles after it, aligned either to the activity of the lBr/lClB (left, contralateral, limb leads) or the rBr/rClB (right, ipsilateral, limb leads). Raster plots, synchronized on the onset of activity of a given muscle, were constructed to visualize the temporal relationships between periods of neuronal discharge and the correlated muscle activity. Rasters were always rank-ordered according to the duration of the burst of ClB/Br in the lead step.

Determining task-related neuronal activity. The methods used to statistically determine the presence, timing and magnitude of changes in discharge activity related to the step over the obstacle are illustrated in Fig. 2, using as an example a cell recorded from the PPC in a previous study (Fig. 5B from Andujar et al, 2010). The discharge activity of this cell demonstrated a clear increase in activity prior to the step over the obstacle for both the left (Fig. 2A) and right (Fig. 2B) lead conditions (PEHs: gray traces).

Initially, we determined whether a cell was *task-related.* To this end, we averaged the cell discharge over all trials (and for both obstacles in cat P2) and divided each step cycle (onset of activity in Br/ClB of one limb until the next period of activity in the same limb) into its 2 component steps, defined as the onset of ClB/Br activity in one forelimb to the onset of the ClB/Br activity in the other limb. Each step was divided into tenths and we calculated the average cell discharge rate in windows of 0.4 steps (~200ms) with the windows being displaced by 0.1 steps (~50 ms) across the period beginning 6 steps before the lead limb onset and ending 1.8 steps after. The average discharge rates calculated by this method are referred to as moving window averages and are illustrated by the red and green traces in Figs. 2A, B. We then used a two-sample, two-tailed t-test to determine whether mean discharge rates in matched windows during the gait modifications were significantly different from control steps. We defined a cell as 'task-related' if the difference in activity was significant ($p < 0.05$) for at least five consecutive windows (~250 ms) during the gait modification in the left or right lead condition. The onset of the change in activity was defined as the center of the first significant window. Significant windows in Fig. 2A, B are indicated by the horizontal shaded bars under the PEHs. We considered multiple periods of significant task-related activity that were separated by periods of < 5 non-significant bins as a single period of modified activity.

In cat P2, in which we used two obstacles of different size, we similarly used the two-sample, two tailed t-test to determine whether cell discharge was influenced by the size of the obstacle. In the example illustrated in Fig. 2C, D there was no significant effect of obstacle size on cell discharge.

Step-advanced vs step-related cells. In previous publications (Andujar J-E *et al.* 2010; Marigold DS and T Drew 2011), we defined cells as step-advanced or step-related depending on whether the earliest change in discharge (with respect to control activity) began, respectively, > or < than 200 ms prior to the step over the obstacle. This was designed to distinguish cells that are more likely related to the planning or preparation of the step over the obstacle from those more likely related to the execution of that step. However, such a general distinction does not differentiate between cells that show transient discharge activity related to one or more steps prior to the step over the obstacle from those that show a prolonged discharge that is independent of any particular step. In the present study, we therefore defined all cells that showed transient changes in discharge activity restricted to a single step as step-related, regardless of whether that change occurred during

a step before or over the obstacle. This allows us to differentiate cells signaling more global aspects of planning from those involved in the planning and/or execution of specific steps.

Condition Selectivity. We next determined if the changes in activity were significantly different in the left and right lead conditions (*condition-selectivity*). As the relative phase of the control activity (activity in the unobstructed locomotion) with respect to the lead limb will be different for the left and right lead conditions for rhythmically active cells (see e.g. Fig. 8A, D-F and Fig. S1), we need to compare the *net activity* in the two conditions (effectively, task-related activity - control activity). To this end, we used a linear regression analysis in which the control and the task-related activity in each condition and for each analysis window (see vertical bar in Fig. 2A) were entered as dummy variables (unobstructed locomotion = 0, task-related activity=1; Fig. 2E). The difference between the mean activity before and during the step over the obstacle and that during the unobstructed cycles provides an indication of the net activity of the cell (plotted in Fig 2F). Regressions in which the slope was significantly different ($p < 0.05$ by t-test) were considered to indicate a significant difference in net activity in the two conditions. When the two slopes significantly differed ($p < 0.05$) for at least five consecutive windows, we classified the discharge as condition-selective. The onset of the condition-selective activity was defined as the center of the first significant window. The illustrated cell did not show a significant difference in the slopes in any window. However, for windows in which there was a significant difference, we then compared the absolute net activity in both conditions and assigned condition selectivity according to whether the net activity was greater in the left or right lead condition. Note that the comparison allows for either increases or decreases in activity to result in the greatest change in absolute net activity.

Modulation of activity during unobstructed locomotion

We used the Rayleigh test for directionality (Batschelet E 1981; Drew T and S Doucet 1991) to determine if cell discharge was modulated (defined as a significant change in activity in a given phase of the step cycle) during the control steps. For those cells with a significant change we also used the circular statistics to calculate a vector (r), that provides an indication of dispersion of the cell discharge. The length of this vector can vary between 0, indicating a completely uniform distribution, to a value of 1, indicating that the cell discharged at the same phase of the step cycle in every step. We arbitrarily used a value of r of ≤ 0.2 to define cells that were weakly or strongly modulated during unobstructed locomotion. For example, the cell in Fig.2 showed significant directional activity in the control trials and was therefore modulated, but the value of r was <0.2, representing the very broad pattern of modulation. In contrast, the cell illustrated in Fig.8A had a value of $r = 0.61$, reflecting the highly modulated pattern of activity.

Alignments used for illustrations

When displaying data from a single condition (left or right lead), we always synchronize to the onset of the activity in the flexor muscle (Br/ClB) of the lead forelimb (e.g. Figs. 2A, B. Fig. S1A,B, and E,F). To compare the cell discharge patterns in the two conditions (left and right lead) we superimpose the activity using one of two methods. For cells that discharge either tonically, or with little evidence of rhythmicity, we superimpose activity from the left and right lead conditions aligned to the onset of the flexor muscle activity in the lead limb, i.e. aligned to the left Br/ClB in left lead and the right Br/ClB in right lead. This allows one to readily appreciate whether cells discharge with the same relationship to the lead limb, regardless of condition (see Fig. S1C and

Fig. 5) or inversely, cells that discharge with different relationships to the lead limb (e.g. Fig. 7). Alignment to the activity in the flexor muscle of the lead limb is also used to examine the condition- selectivity as in Figs. 2, 10B, 11F. However, in cells that show strong rhythmicity during unobstructed locomotion, superimposing activity aligned to the flexor activity of the lead forelimb makes it difficult to appreciate the step-related activity of the cells (see Fig. S1G). Therefore, in such cells, we aligned activity to the lClB/lBr for both the lead and trail conditions (Fig. S1H, see e.g. Fig. 8 and Figs. 11D, E).

Histology. At the end of the series of experiments, the cats received the same premedication as for the initial surgery and were then deeply anesthetized with an intravenous injection of pentobarbital sodium (Somnitol, 30mg/kg) and perfused *per cardia* with a formaldehyde solution. The brain was removed and photographed. The rostral part of the cerebral cortex, containing the entire cruciate sulcus, was sectioned in the parasagittal plane (40 μm) and stained with cresyl violet. To accurately localize recorded neurons, we calculated the location at which each penetration crossed layer V of both banks of the cruciate sulcus. The anteroposterior coordinate of each recorded neuron was calculated as the linear distance of the cell from the fundus of the cruciate sulcus as measured along the length of the straightened layer V (Jiang W and T Drew 1996; Andujar J-E and T Drew 2007). The medio-lateral coordinate of the cell was based on the laterality of the section that included the recorded site. These two coordinates were used to plot the location of each cell on a flattened map of the cortex centered on the fundus of the cruciate sulcus (see Fig. 3). Cytoarchitectonic borders were determined based on the criteria detailed in previous studies (Hassler R and K Muhs-Clement 1964; Avendano C et al. 1988; Ghosh S 1997b).

Anatomical Experiments. Retrograde tracing experiments were performed on 4 cats (weights: 4.6-7.4 kg), different from those used in the electrophysiological experiments. Cats were anaesthetized using the same procedures as described above and a craniotomy performed to expose the cortical region between the ansate and the cruciate sulci. A glass-insulated tungsten microelectrode (0.5-1.0 MΩ) was then inserted into the cortex at coordinates designed to traverse area 6iffu in the ventral bank of the cruciate sulcus at distances from the mid-line that corresponded to those from which cell recordings were made (see Table I). As the electrode was lowered, we recorded neuronal activity to identify the different cell layers that we traversed as well as the cruciate sulcus. When we crossed the cruciate sulcus, we advanced the electrode until relatively large action potentials were recorded, approximately 1.5 mm from the sulcus. We assumed that this marked layer V of area 6iffu and the depth of this layer with respect to the cortical surface was noted. The procedure was then repeated at different rostrocaudal or mediolateral coordinates to provide a profile of the region of cortex of interest. We then introduced a 32-gauge needle attached to a Hamilton syringe at the targeted coordinates and lowered it to the previously-noted depth of layer V of 6iffu. Injections of tracer (either Texas Red, Alexa Fluor or Fast Blue) were then made by using a Harvard Apparatus injector system. After waiting 5 minutes for stabilization, between 0.2 and 0.3 μl of tracer were injected at a rate of 0.1 μl/min. One to three injections were made at each coordinate (see Table I). In sites, in which multiple injections were made, the injection needle was left in place for 5 mins after each injection. This resulted in labelling across all six cortical layers (see Fig. 12). At the end of each series of injections the needle was left in place for 5 mins before being raised. If multiple injections were made in a cat, the entire process was repeated for the next coordinate.

Following the injections, the cortex was covered with Gelfoam and a thin layer of dental acrylic before closing the skin. Analgesic and antibiotic procedures were as above. After a transport period of 13-21 days, cats were deeply anaesthetized and perfused *per cardia* with a solution of 4% paraformaldehyde in phosphate buffer (4°C, pH 7.4; see Andujar J-E and T Drew 2007 for details). The brains were cryo-protected and blocks containing the parietal and frontal cortices sectioned in the parasagittal plane at a thickness of 40μm. Every third section was mounted for fluorescent analysis and the adjacent section stained with cresyl violet.

Sections mounted for fluorescent microscopy were examined at a magnification of 100X and the location of labelled cells marked using the Neurolucida system (MBF Bioscience). We also used the Neurolucida system to trace the contours of the surface of the brain and layer V, as well as to mark the locations of the fundi and the rostral and caudal boundary of different sulci. These data were used to make flattened maps of the peri-cruciate cortical regions as described previously (see Jiang W and T Drew 1996; Andujar J-E and T Drew 2007). In brief, the flattened layer V was divided into 200μm bins and the number of labeled cells in each bin was counted. The relative location of each bin was then calculated with respect to either the fundus of the cruciate sulcus (Cru) or to the most rostral aspect of the splenial sulcus (Spl) in the same way as for the location of the recording site (see above). Cells dorsal and caudal to Cru were assigned positive values, while cells ventral and rostral to Cru were assigned negative values. With respect to Spl, positive values were assigned to cells dorsal and caudal while negative values were assigned to cells that were ventral and caudal.

To plot contour plots we calculated the mean and Standard deviation (SD) of the total number of labelled cells in the region of interest. We then set the maximum value for the number of cells in a bin to this mean+SD. This had the effect of reducing the power of bins in which there were an excessive number of labelled cells (Andujar J-E and T Drew 2007).

Results

Database. We present data on the characteristics of PMC neurons recorded within the ventral bank of the cruciate sulcus, within areas 6iffu, 4fu, and the adjacent area 4δ (Fig 3). Within this region, we recorded 281 neurons (104 in P1 and 177 in P2) from 71 electrode penetrations (25 in P1 and 46 in P2); these neurons formed our initial database. Of these, visual inspection showed that 72/281 cells were clearly unrelated to the task and our off-line analyses revealed that an additional 46/281 cells showed no task-related activity during the steps leading up to, or during, the step over the obstacle. These 118 (72+46)/281 neurons were not treated further. An additional 27 cells were recorded for fewer than 4 steps over each obstacle in each condition and were likewise removed from further quantitative analysis.

The remaining 136 task-related neurons (22 in cat P1 and 114 in cat P2) comprise the final database used in this report. The 22 cells in cat P1 were recorded from 13 penetrations that were all located within area 6iffu. In cat P2, 81/114 cells were recorded from 30 penetrations in area 6iffu and 2 penetrations in area 4fu; 33/114 neurons were recorded from 8 penetrations in adjacent area 4δ. Because area 4δ is also found in the caudal (dorsal) bank of the cruciate sulcus, we refer to the region that we recorded in the rostral (ventral) bank as 4δr as in the study of Ghosh (Ghosh S 1997b, 1997a). The location of the penetrations from which cells used in this report were recorded is illustrated in Fig. 3.

Of the 136 task-related cells, 48/136 were identified as corticofugal cells by antidromic activation from the stimulating electrodes in the PT or CP while a further 64/136 were recorded near (generally < 200μm) an antidromically activated cell. The other 24/136 cells were classified as being in layer V based on the appearance of larger action potentials ~ 1.5mm after crossing the cruciate sulcus. In terms of areal representation, 31/103 (30.1%) of cells recorded in areas 6iffu and 4fu were identified as corticofugal cells, compared to 17/33 (51.5%) of cells in area 4δr.

As our analysis showed no difference in the characteristics of the cells recorded from the 2 penetrations in area 4fu and those in area 6iffu, area 6iffu in the text that follows also includes 4 cells from area 4fu.

General Characteristics

Activity during unobstructed locomotion: control task

In area 6iffu, most of the neurons recorded (79/103, 76.7%) showed no significant modulation of their discharge activity during unobstructed locomotion. Of the remaining 24/103 modulated cells, only 11 (11/103 = 10.6%) showed a vector (r) value of $r > 0.2$, which we use as an arbitrary division for a strongly modulated cell. In contrast, most cells in area 4δr, 24/33 (72.7%) were modulated during unobstructed locomotion and 18 of these (18/33 = 54.5%) were strongly modulated.

Period of task-related activity

Our database of 136 task-related neurons showed a wide range of activity patterns during steps over the obstacle, as illustrated in Fig. 4A, B for the left lead condition. At the most general level, this population appears as a continuum of cells, with some cells modifying their discharge (indicated as either an increase, black bars, or a decrease of activity, gray bars) several steps before the step over the obstacle, while others modified their discharge only later, during the step over the obstacle by the lead forelimb, or even after the passage of the lead forelimb. Other cells (N=15 in cat P2) showed no modification of activity during the left (contralateral limb) lead condition but

showed task-related activity during the right lead condition. At a population level, progressively more cells showed task-related activity as the obstacle advanced towards the cat with the greatest percentage of cells being active just before and during the step over the obstacle (Fig. 4C). Note that despite the fact that the obstacle became visible to the cat 10-12 steps before it stepped over the obstacle, all except one cell began to discharge less than 4 steps before the step over the obstacle. Despite the apparent continuity of cell onset times, in the following sections we propose that several different cell populations can be identified, each with well defined characteristics and separate functions. To emphasize the sequential nature of the transfer of information within the premotor cortex, in the sections that follow we identify these different populations, beginning with those that discharged earliest, prior to the step over the obstacle, and continuing through to those that discharged latest, during the passage of the hindlimbs.

Size selectivity

Out of the population of 114 cells recorded from cat P2 and showing task-related activity in at least one of the two conditions (left and right lead), 10/98 (10.2%) of cells showing task-related activity in the left lead condition showed an effect of obstacle size, as did 14/113 (12%) cells showing task-related activity in the right lead condition; only 2 of these 24 cells showed an effect in both conditions. The effects were mixed in both the left and right lead conditions, with the larger obstacle resulting in an increase in activity in 16/24 cases but a relative decrease in the other 8/24 cases. Changes in activity generally occurred for only a part of the total range of the period of task-related activity.

Activity during voluntary gait modifications

Step-advanced cells

The largest division of cells comprised 86/136 neurons that modified their discharge > 200ms prior to the onset of the step over the obstacle by the lead limb and that showed a sustained change in discharge activity (Table II). These step-advanced cells showed periods of task-related activity that endured for > 0.5 step cycles (1 step). In 78/86 (90.7%) cells, discharge activity was tonic (not significantly directional) during unobstructed locomotion.

Within this major division, we identified two populations of cells. In one population, the profile of cell discharge was similar in both the left and right lead condition and cell discharge ended almost at the same time, with a difference of less than one step relative to the onset of the step over the obstacle in the lead limb. These cells were defined as limb-independent (64/86, 74.4%). The other population showed a similar profile of activity during the left and right lead conditions until just before or during the step over the obstacle, whereupon discharge continued until the step over the obstacle only in one condition. These cells were defined as limb-dependent (22/86, 25.6%). Cells of each population were intermingled and found throughout area 6iffu, as well as in area 4δr (Fig. 3A, B).

Step-advanced, limb-independent cells.

Limb-independent cells were the largest population within the step-advanced division and task-related activity in most cells was similar in the left and right lead conditions (see Fig. 5). Most cells discharged similarly to those illustrated in Fig. 5A-D in that they showed an increase in activity that began several steps before the step over the obstacle and showed a ramp, or sustained, increase of activity that continued until either the end (e.g. Fig. 5A,B) or the onset (e.g. Fig. 5C,D)

of the step over the obstacle. This was the most common pattern of activity with 28/64 cells showing a simple monotonic increase in discharge; a further 12/64 cells showed a simple monotonic decrease that ended at the time of the step over the obstacle or just after it. However, several variations were observed in this population. In particular, a small population of cells discharged either with an initial increase prior to the step over the obstacle and then a reciprocal decrease of activity (N=4, example in Fig. 5D) or with the inverse pattern, a decrease followed by an increase (N=4, see Fig. 9A). Eight (8/64) cells continued to discharge until the passage of the hindlimbs over the obstacle; these cells are treated in a separate section (below). A further 7 cells stopped discharging 1 step prior to the step over the obstacle (Fig. 5E) and a single example stopped discharging 1 step cycle (2 steps) prior to the step over the obstacle (Fig. 5F). Note that tonic activity was observed during unobstructed locomotion (blue traces) in all of these illustrated examples.

Details on the timing of the task-related activity for this step-advanced, limb-independent population of cells are provided in Fig. 6. Fig. 6A illustrates the discharge activity of all 64 limb-independent cells in the left lead condition, rank-ordered either to the time of the earliest onset of cell activity (left panel) or to the end of the initial period of discharge (right panel). In all except one cell, the earliest sustained modification of activity began 3-4 steps (~2 step cycles) prior to the step over the obstacle (Fig. 6A). Fig 6B plots the percentage of cells that were either facilitated (black line) or suppressed (gray line) at different times before and during the step over the obstacle. It shows that in both the left (*top* panel) and right (*bottom* panel) limb lead condition, population activity peaked ~ 1step before the step over the obstacle and then declined following the step over the obstacle.

The temporal relationship between the periods of task-related cell activity during the left and right lead condition, for both the onset and the offset of task-related activity, is illustrated in the scatterplots in Fig 6C, D. For these graphs, onset and offsets of task-related activity were calculated as the time that the burst of activity crossed the 99% interval of confidence of the standard error of the averaged control activity. This provided a greater resolution than provided by the moving window averages.

We first detail the timing relationships of the offset of the task-related activity, as we use this to indicate whether cell discharge is better related to the placement of the paw in front of the obstacle, to the passage of the forelimb over the obstacle or to the passage of the subsequent hindlimb. As would be expected based on the criteria for inclusion in this group, the timing of the offset of the initial period of task-related activity was very similar in both conditions, as indicated by the proximity of the points to the line of equivalence (Fig. 6C). The color of the symbols in the scatterplots identifies groups of cells that are defined by their phase of offset with respect to changes in the periods of EMG activity in different limbs. We define 3 main periods of activity. The major period (green symbols) is defined as occurring between the end of the period of activity in the flexor muscle of the right ipsilateral limb (rClB-1_off) as it is positioned in front of the obstacle (plant limb) and the onset of activity in the semitendinosus (lSt on) in the lead (homolateral) hindlimb serving to bring the hindlimb over the obstacle. This period therefore encompasses all those cells in which the end of the period of activity occurs just before, during, or just after the passage of the lead forelimb over the obstacle, including cells with properties similar to those of Fig. 5A-C. The red and salmon-colored symbols indicate cells in which activity

continued past both the passage of the forelimb and the subsequent onset of activity in the lead hindlimb. Of these, the cells with a red symbol exhibited a simple increase or decrease of activity before the passage of the lead forelimb and continued until the phase indicated by the symbol. In contrast, the salmon-colored symbols indicate cells discharging similarly to those in Fig. 5D with reciprocal activity before and after the passage of the lead forelimb. Cyan symbols indicate cells in which the end of the discharge occurred prior to the positioning of the plant limb. The cell in Fig. 5F is indicated by the blue symbol.

The difference in the time of the offset of the task-related discharge in the left and right lead conditions varied by less than 1 step, as indicated by the inclusion of all points within the two dotted lines as well as by the histogram detailing the difference in the timing in the two conditions (Fig. 6E). As determined by our definition of limb-independent, all cells showed a phase difference of < 1 step (mean = 0.02± 0.26, standard deviation: SD).

While the end of the period of discharge was constrained by the definition for inclusion as a limb-independent cell, there was no such constraint for the time of the onset. However, the scatterplot and histogram of Figs. 6D, F indicate that the onset of the earliest discharge in most cells also began at a similar phase before the onset of the step over the obstacle in the lead limb in both the left and right lead conditions (mean = -0.18 ± 0.56SD). As activity in the two limbs is out of phase by 0.5, this dictates that the onset of activity in most cells was independent of the period of EMG activity in the lead limb. This can also be appreciated by inspection of the data in Fig. 5, which shows that the pattern of the task-related activity superimposes while the activity in the left and right flexor muscles alternates. There was, however, a tendency for cells to discharge slightly earlier in the left lead condition (negative values) than in the right lead condition (positive values) (Fig. 6F).

Step-advanced, limb-dependent cells

This second, smaller, sub-division (N=22) of the step-advanced cells was defined based on the temporal distinction between the offset of the activity in the left and right lead conditions. This population was more heterogenous in nature. The largest grouping within the population included those cells in which the task-related activity continued until the step over the obstacle in one condition but stopped one step before the step over the obstacle in the other condition. An example is illustrated in Fig. 7A. In the left lead condition (*top panel*), there was an increase in discharge activity that began ~3 steps before the onset of the step over the obstacle and that continued until the onset of the step over the obstacle. In the right lead condition (*middle panel*), the onset of the modification in discharge occurred at a similar time relative to the onset of the step over the obstacle but the cell showed a large increase as the left limb was brought forward and placed (planted) on the ground prior to the step over the obstacle with the right forelimb. Note that in both the left and right lead condition, the offset of cell activity is modified with respect to the activity in the left, contralateral, limb. Three other cells discharged in a qualitatively similar manner and 2 additional cells discharged only with respect to the placement of the left limb in front of the obstacle in the right lead condition. Three other cells showed the reciprocal pattern of activity to that in Fig. 7A, namely one in which cell discharge was related to the placement of the paw of the right, ipsilateral, limb when it was placed in front of the obstacle. An example of this is illustrated in Fig. 7B.

Several other limb-dependent cells showed their major difference in discharge activity just before or during the step over the obstacle. The cell in Fig. 7C, for example, showed a large increase in activity during the step over the obstacle in the left lead condition (*top panel*) that is missing in the right lead condition (green trace in the *bottom panel*). Such a pattern was observed in 3 other cells, including the example in Fig. 7D. In both examples, but particularly that in Fig. 7D, one can also see a modulation in the cell discharge that occurs during the period of swing of the left (contralateral) limb in both the left and right lead conditions. In the left lead condition, the final burst occurs during the step over the obstacle; in the right lead condition discharge decreases subsequent to the placement of the left limb prior to the step over the obstacle by the right (ipsilateral) lead limb. Other cells showed task-related activity only during the step over the obstacle with the left limb (N=6) or, conversely, only during steps over the obstacle with the right limb (N=3).

As expected, based on their classification as limb-dependent, cells that modified their discharge activity in both conditions tended to have a difference of ~ 1 step between their time of offset in the 2 conditions. As such, in the plot of the time of offset (Fig. 7E, *left*), symbols tend to lie on one of the dotted lines to either side of the line of equivalence, rather than lying on that line as for the limb-independent cells (Fig. 6C). However, the onset of the change in discharge did lie on the line of equivalence (Fig. 7E, *right*) in most, although not all, cells. This suggests that the cells begin to modify their discharge activity at a similar time before the step over the obstacle but that the offset differs depending on whether they step over the obstacle with the left or right limb.

Step-related cells

The other major division of cells was the step-related cells (N=41/136) that showed changes in activity either immediately before or during the step over the obstacle, or that showed a discrete change in activity in the steps preceding the step over the obstacle (Table II). During unobstructed locomotion some of the step-related cells showed strong, rhythmical, step-by-step modulation of activity (N=22) while others showed either weak rhythmicity or a tonic background (N=19). Qualitatively, there was a clear difference in cells showing a strong rhythmical discharge ($r > 0.2$) and those that were only weakly or not modulated (≤ 0.2). These cells were intermingled with each other and with the step-advanced cells (Fig. 3C) although there was a tendency for most strongly-rhythmically active cells to be located within area 4δr. Within this population, 32/41 cells modified their discharge activity discretely, either during the steps prior to and/or during the step over the obstacle by the forelimb. The other 9/41 cells (described later) modified their discharge either between the passage of the forelimbs and the hindlimbs over the obstacle or during the passage over the obstacle by the hindlimbs (Table II). Although rhythmically modulated cells are a minority in this report, it should be noted that only relatively few penetrations were made in the more lateral regions in which these cells predominated and none of the penetrations presented in this manuscript were made in area 4γ (generally considered to correspond to MI) in which rhythmically active cells predominate (Drew T 1993; see Fig. S2).

Figs 8A, B illustrate 2 cells that showed step-related increases in activity during the step over the obstacle with the left, contralateral, forelimb in the left lead condition. As such, these cells show changes in discharge activity that are commonly associated with the activity of cells in area 4γ (Drew 1993). In A, the activity is superimposed on weak modulation during unobstructed locomotion, while in B, the cell was mostly quiet, except during the step over the obstacle. The

neuron illustrated in Fig. 8C shows a very different pattern of activity from that illustrated in Figs. 8A, B. During the step over the obstacle in both the left lead (red trace and red arrow, L) and right lead (green trace, green arrow, R) condition the cell did not discharge at all. However, in the right lead condition, the cell discharged in the step before the step over the obstacle when the left, plant, limb was placed in front of the advancing obstacle (cyan arrow, LP) prior to the step over by the right limb. The cell thus had a similar relationship to the plant limb as those illustrated in Figs. 5E and 7A,B. The apparent difference in the time of discharge is caused by the difference in the method of alignment in this figure in which all data are aligned to the onset of activity of the lClB during the step over the obstacle in both the left and right lead conditions, and not to the ClB of the lead limb, as in Figs. 5 and 7 (see Methods and Fig. S1). As such, in the right lead condition (green trace) the period of activity in the rClB during the step over the obstacle precedes the activity of the lClB in the left limb, which is the second to pass over the obstacle (trail limb, see arrows and EMG traces below Fig. 8C).

The rhythmically-active cells illustrated in Figs. 8D, E, also showed an increase in discharge related to the left, plant limb in the right lead condition (green traces). However, these two cells additionally showed task-related activity during the step over the obstacle by the left, contralateral, limb in the left lead condition (red traces). In both cells, as for the other 3 cells in this figure, increases in cell discharge were always related to the left, contralateral, limb.

Last, there were a very few (N=2) cells that discharged after the period of activity of the left forelimb flexor in the left lead condition (Fig. 8F, red trace), but prior to this period of activity in the right lead condition (Fig. 8F, green trace). We suggest that such cells could be involved in the coordination between the passage of the two forelimbs over the obstacle.

Two other cells showed significant changes in activity in the steps preceding the step over the obstacle in the left lead condition.

Forelimb-hindlimb cells

In total, including both step-advanced and step-related cells, 25/136 neurons had a period of discharge that continued until the passage of one or more of the hindlimbs over the obstacle (Table II), either together with, or in the absence of, forelimb-related changes in activity. This included 16/86 step-advanced cells (red and salmon-colored circles in Fig. 6C) and 9/41 step-related cells.

In one half of the step-advanced cells (8/16), there was a period of prolonged task-dependent activity prior to the step over the obstacle and then another, reciprocal, period of task-related activity beginning with the passage of the forelimb over the obstacle and continuing until the passage of the hindlimbs (Figs. 5D, 9A). For example, in the cell illustrated in Fig. 9A (*top panel*), there was a limb-independent decrease in activity prior to the step over the obstacle followed by a prolonged increase in activity that continued after the step over the obstacle by the forelimbs until the passage of the hindlimbs over the obstacle. This activity continued almost to the passage of the second hindlimb to step over the obstacle (vertical dotted line). This relationship is better seen in the *middle* and *bottom* panels of Fig. 9A in which the activity during the left and right lead conditions, respectively, is illustrated separately. Activity during the left lead condition (*middle* panel) is synchronized to the onset of the right, ipsilateral, hindlimb flexor (rSrt), while that during the right lead condition (*bottom* panel) is synchronized to the lSrt (contralateral hindlimb flexor).

In both panels, one can clearly observe the continuation of the discharge to the time of passage of the hindlimbs over the obstacle. Similar patterns of activity were observed in the 7 other step-advanced, limb-independent cells with this general type of pattern.
The other 8/16 step-advanced cells showed either a monotonic increase in activity (N=6) or a monotonic decrease in activity (N=2) that began before the step over the obstacle by the lead forelimb and continued until passage of the lead hindlimb (red circles occurring after "St_On" in Fig. 6C).

A variety of patterns were seen in the 9 step-related cells that modified their discharge during the passage of the hindlimb over the obstacle. In the example of Fig. 9B the cell modified its discharge activity only in the left lead condition and only later, after the passage over the obstacle by the left forelimb (*top* panel). This period of discharge is related to the period of activity in the semitendinosus of the right hindlimb (rSt), corresponding to the last leg in the sequence of four that stepped over the obstacle. This relationship is better seen in the illustration of the *bottom* panel of Fig. 9B in which the cell activity is aligned on the rSt. The example of Fig. 9C shows a more complex pattern of activity in which the cell showed limb-independent activity during the passage of the lead limb but also exhibited 2 other periods of (limb-independent) increased activity subsequent to that, with the last period occurring during the passage of the hindlimbs over the obstacle. The complex patterns of activity in these cells should be contrasted with the relatively simpler patterns of discharge observed in M1 (Drew T 1993; Widajewicz W et al. 1994).

Condition Selectivity
To determine the extent to which cell discharge varied between the left and right lead conditions we calculated the condition-selectivity of the cell discharge (see Methods). This measure determines how changes in net activity in one condition differ from changes in the other condition, independent of whether the activity is significantly different from control. Altogether, 53/127 classified cells (Table II) showed condition-selective responses. Because in cat P2, we used obstacles of different sizes, we also used a 2-way ANOVA to determine if there was any interaction between size and condition. Such an interaction was observed in only 4/47 cells showing condition selectivity in this cat.

In general, differences in net activity during the left and right lead conditions were least for the step-advanced, limb-independent cells and greatest for the rhythmically-active, step-related cells (Fig. 10). The changes in activity patterns observed during left lead for all the task-related cells included in one of our four major groups (see Table II) are illustrated in Fig 10A while plots of the net activity for 4 example cells (see legend) are illustrated in Fig. 10B-D.

As indicated in Fig. 10Ci, only 19/64 (29.7%) of the step-advanced, limb-independent cells showed any significant differences in net activity between the left and right lead condition. In most of these cases, condition-selectivity was transient, and occurred only during small parts of the total period of task-related activity, as illustrated for the example in Fig. 10Bi. On a population basis, major differences in activity for both conditions slightly increased 1 step before the onset of the step over the obstacle (Fig. 10Di). Thus, although most limb-independent cells were task-related 1 step before the step over the obstacle in both the left and right lead conditions, some of this population was beginning to distinguish between the two conditions.

As might be expected, condition selectivity was much more prevalent in the step-advanced, limb-dependent cells (11/22 cells, 50%) and was present both before and after the onset of the step over the obstacle (Fig. 10Cii). While, intuitively, one might expect all limb-dependent cells to show significant condition-selectivity, the current analysis determines differences between the net activity in the two conditions (see Fig. 2). For example, in Fig. 10Bii, net activity in the right lead condition is significantly greater than that in the left lead condition at the beginning of the task-related period of activity while net activity in the left lead condition is significantly greater than that in the right lead condition during the step over the obstacle. Indeed, the data in Fig. 10Dii are compatible with the cell discharge patterns illustrated in Fig. 7 in that the population activity shows increased net activity just prior to and during the step over the obstacle in the left lead condition and a similar increase that peaks one step before the obstacle in the right lead condition. This is compatible with a bias towards regulating activity in the contralateral (left) limb in both conditions (in the left lead condition as it steps over the obstacle and in the right lead condition when it is the plant limb).

Relatively modest condition selectivity (7/19, 37%) was observed in the step-related cells with tonic discharge during unobstructed locomotion (Fig. 10C,Diii). All of these cells were related to the forelimbs and no condition-selective changes were observed in the 8 hindlimb-related cells in this group.

The major group of cells showing condition-selectivity was that containing the cells that showed strong rhythmicity during unobstructed locomotion (16/22, 73%). Many of these cells showed multiple periods of condition-selectivity before and during the step over the obstacle, as in the illustrated example (Fig. 10Biv). As for the step-advanced, limb-dependent cells (Fig 10C,Dii), rhythmically-active cells showing greater net activity in the left lead condition were preferentially active during the step over the obstacle with the left, contralateral limb. On the other hand, greater net activity in the right lead condition was mostly frequently observed one step before the step over the obstacle (Fig. 10 C,D iv). Again, this speaks to an effector-specific regulation of the left (contralateral) limb.

Receptive Fields and Microstimulation.

Receptive fields (RF) were tested for 78/127 of the cells classified as step-advanced or step-related (Table II). With respect to step-advanced cells, 40/48 cells for which a RF was found responded to movement of an object across the visual field with 19/40 of these cells responding to a looming stimulus. Only 4 cells were found to have a somatic RF. In contrast, 13/22 step-related cells had a RF on the limbs while the other 9/22 responded to visual stimuli, including looming. In terms of sub-region, 8/22 (36.4%) cells for which a RF was examined in area 4δr had a somatic RF compared to 8/78 (10.3%) in area 6iffu. Visual receptive fields (including looming) were found in 6/22 (27%) cells in area 4δr and 43/66 (65%) in area 6iffu.

Microstimulation was applied in layer V of 6iffu in 10/13 tracks in which task-related cells were recorded in cat P1 and in 27/32 tracks in cat P2. The ICMS was ineffective at 100μA in 29/37 tracks. In the other 8 tracks, ICMS produced head movement in 5 tracks (threshold = 100μA, N=4; 50μA, N=1) and weak, slow, forelimb movements in the other 3 tracks (threshold 75-100μA). ICMS in area 4δr was applied in all 8 tracks in this region; responses were evoked in the forelimb

from 4 tracks (thresholds 25-50μA) and in the hindlimb from 1 track (threshold = 75μA); no effects were evoked from 3 tracks at 100μA.

Comparison with cells in the PPC and M1

Some of the characteristics of the cells that we recorded in these subregions of the PMC resemble those that we have previously described for the PPC (Andujar J-E *et al.* 2010; Marigold DM and T Drew 2017) and M1 (Drew T 1993; Drew T *et al.* 2008). For example, we have previously found both step-advanced and step-related cells in areas 5a and 5b of the PPC and these cells showed a variety of different patterns during the gait modification. In M1, we have described cells that show step-by-step modulation during unobstructed treadmill locomotion together with brief changes in discharge activity during the step over the obstacle (Drew T 1993; Yakovenko S and T Drew 2015).

To compare the general characteristics of the populations in the PPC and the PMC, we first calculated the phase of activation of the populations of cells recorded in the studies referenced above by using the same methods as for the PMC cells (see Fig. 2 and Methods). The resulting phase diagram (Fig, 11A) shows the same general distribution of cell patterns as we found for the PMC (Fig. 4A) with some cells starting to discharge several steps in advance of the step over the obstacle (step-advanced) while others discharged later, just before, or during, the step over the obstacle. However, although very similar, the cells in the PPC discharged significantly later (Kolmogorov-Smirnov test, $p < 0.01$) than those in the PMC. This is shown in Figs. 11B, C in the form of cumulative histograms of the cell onset for all cells recorded in each population (Fig. 11B) as well as only for those that were step-advanced (Fig. 11C).

In our previous studies on the PPC, we concentrated on two issues, namely the general characteristics of cells in this region (Andujar J-E *et al.* 2010) and the relationship between the onset of activity in cell discharge and the location of the obstacle (Marigold DM and T Drew 2017). However, in the context of this present study, we re-examined our previous database of forelimb-related PPC cells to determine whether similar cell types to those described in Figs. 5-10 were included among our PPC population. We found similarities as well as some differences. The most obvious similarity was the presence of a large population of step-advanced, limb-independent cells in both cortical regions. An example of such a cell from the PPC is illustrated in Fig. 2. With respect to differences, in addition to the relatively later onset of the change in activity in the PPC (Fig. 11C), we did not find step-advanced cells in the PPC that showed discharge patterns similar to those illustrated in Fig. 7, namely the step-advanced, limb-dependent cells.

With respect to the step-related cells, a large proportion of forelimb-related cells in both the PMC and in the PPC showed significant changes in their discharge activity before or during the step over the obstacle in both conditions (PMC: 35/41, 85%, left lead; 36/41, 88%, right lead. PPC: 42/44, 95% left lead; 39/44, 89%, right lead). However, there were differences in the temporal pattern of the condition-selectivity of the two populations of neurons with respect to the lead limb. As illustrated in Figs. 10Diii-iv, a substantial proportion of PMC cells increased net activity during the step over the obstacle in the left lead condition (red trace) while in the right lead condition, the population showed greater net activity in the step before the obstacle, as the left, contralateral limb was placed on the treadmill belt prior to the step over the obstacle (green trace). A large proportion of the PPC cells likewise exhibited significantly increased periods of net activity during the step over the obstacle in the left lead condition (red traces in Figs. 11F,G). However, in the right lead condition, significant increases in net activity were mostly observed as the left contralateral limb

followed the right limb over the obstacle (as the trail limb). As such, when the traces are synchronized to the lead limb (Fig. 11F.G), the increase in significant net activity in the right lead condition (green trace) trails that in the left lead condition (see also individual example in Fig. 11D,F), rather than preceding it as for the PMC population. In contrast, only 2 cells in the PPC showed increased activity in the step preceding the step over the obstacle in the right lead condition (one example illustrated in Fig. 11E).

Application of the same methods to a population of motor cortical cells recorded from the forelimb representation of 2 cats during a previous study (Yakovenko S and T Drew 2015) showed the presence of a large proportion of cells showing brief periods of discharge just before and during the step over the obstacle in both the left lead and right lead (the latter referred to as trail in previous publications) condition (Fig. S2). This pattern of activity reflects the fact that motor cortical cells, in both the left and right lead conditions, discharge in relationship to the specific changes in the pattern of muscle activity required to step over the obstacle (Drew T 1993). However, in general, and when comparing the entire population, greater changes in net activity during the left lead condition were observed primarily during the step over the obstacle by the lead, contralateral, limb (Fig. S2G). Cells showing greater net activity in the right lead condition were most active ~ 1step before and 1 step after the step over the obstacle by the lead, ipsilateral, limb (green trace). The latter of the two peaks represents cells discharging prior to and during the step over the obstacle by the contralateral limb (as for the PPC cells, Fig. 11D,F) while the former represents cells discharging to the contralateral limb in the step preceding the step over the obstacle by the right limb. In the right lead condition, some of these cells showed changes in activity related to the plant limb, as in the PMC.

Cortico-cortical connections

We analyzed data from 5 injections in 4 cats (Table I), in 3 of which the tracer was entirely restricted to area 6iffu, while in one there was some spread into area 4fu, and in another there was some leakage into the dorsal bank of the cruciate sulcus. In all cases, the injections were made in the same regions from which we recorded unit activity. Fig. 12A-D shows 4 representative sections from 1 cat in which 2 different tracers were injected into area 6iffu at two different lateralities. Both injections resulted in heavy retrograde labelling in several cortical areas, including particularly, adjacent areas of 6iffu, the ventral aspect of the posterior cingulate cortex, and areas 6aα and 6aβ. There was also labelling in area 5b (Fig. 12B) and in the more rostral parts of area 7 of the PPC, around the lateral gyrus (Fig. 12C), especially from the most medial (Texas Red) injection. Weak labelling was also observed in area 4δr, in area 4fu, in area 6aγ, and in the prefrontal cortex. Note that retrogradely-labelled cells were observed in both the more medial and lateral regions of area 6iffu following the Fast Blue injection suggesting a bidirectional transfer of information within this area. However, few cells were located in more lateral regions of the cruciate sulcus following the most medial injection suggesting little transfer of information from more lateral to more medial regions. Note also that the cells labelled in the posterior cingulate cortex from the two injections in area 6iffu formed multiple, but non-overlapping populations, in both the dorsal and ventral banks of the splenial sulcus.

The distribution of the labelling is quantified in Fig. 13 which shows density plots of the distribution of the labelled cells from the example illustrated in Fig. 12, The contour plots of Fig. 13E,F clearly show 3 areas of dense labelling. First, there is a concentration of labelled cells within

area 6iffu that extends into the adjacent areas 6aα and 6aβ. Second, there is a concentration of labelling caudal to the ansate sulcus, in area 7 and to a lesser extent in area 5b that is largely within the forelimb representation (see Andujar and Drew 2007). Lastly, there is a concentration of labelled cells in the cingulate cortex. There is also weak labelling in 4δr and in the more lateral regions of the dorsal aspect of 4δ. Noticeably, there was very little labelling in areas 6aγ or 4γ (MI). In the injection that extended into area 4fu, we observed no qualitative difference in the extent of the labelling.

Discussion

We report that cells in areas 6iffu and 4δr of the feline premotor cortex show task-related changes in discharge activity during the performance of visually-guided, voluntary gait modifications. The cells showed two principal patterns of activity, either discharging for several steps before the step over the obstacle (step-advanced cells) or discharging discretely during a single step, before, during, or after the step over the obstacle by the forelimb (step-related cells). The characteristics of this discharge activity are compatible with a role for the cat PMC in planning gait modifications and suggest parallels with the contribution of the PMC to the planning of voluntary movement in primates. During locomotion, we propose that the different cell populations within the PMC provide a neuronal substrate that participates in the temporal transformation of a global signal providing information about the presence of an obstacle into one that specifies the pattern of muscle activity required to negotiate that obstacle.

Areas 6iffu and 4δr as part of a feline premotor cortex

Areas 6iffu and 4δ, by definition, are part of area 6 and area 4, respectively, based on their cytoarchitecture (Hassler R and K Muhs-Clement 1964; Ghosh S 1997b). Each has distinctive connections with other regions of areas 4 and 6, as well as adjacent sensorimotor cortical areas (Ghosh S 1997a, 1997d), but information on neuronal activity during behavior is lacking. Consequently, it has been difficult to attribute functions to these regions or to equate them with premotor areas in primates (although see Ghosh S 1997c, 1997a, 1997d).

In the case of area 6iffu, it has been suggested that in its most medial part it forms part of an oculomotor control region. One study (Guitton D and G Mandl 1978), for example, has described that microstimulation of the most medial region of the ventral bank of the cruciate sulcus produces saccadic eye movements and Olson has likewise suggested these same regions have a visual or oculomotor function (Olson CR and I Jeffers 1987; Olson CR and K Lawler 1987; Olson CR and SY Musil 1992b). Olson (Olson CR and I Jeffers 1987) additionally showed that injections of tracer into the most medial parts of 6iffu (area 6m) resulted in strong retrograde labelling of posterior regions of area 7 (see also Olson CR and K Lawler 1987), known to have visual input, as well as in parts of cingulate cortex that equally have been identified as having oculomotor and visual functions (Olson CR and SY Musil 1992b, 1992a).

We also found a concentration of retrogradely labelled neurons in area 7 from our injections, but these were localized to more rostral regions of area 7 (Fig. 12C) than those labelled in the studies of Olson (Olson CR and I Jeffers 1987). Moreover, the labelling extended rostrally into area 5b, an area more likely to be implicated in somatomotor control than in oculomotor control (Olson CR and I Jeffers 1987; Olson CR and K Lawler 1987). We also failed to observe saccadic eye movements to stimulation from any of the sites that we examined, and the cells that we analyzed in this region clearly discharged in relationship to the motor activity of the cat. Taken together, this suggests that most of our recordings were in regions of the ventral bank outside the oculomotor region in the most medial part of 6iffu. This is further supported by the fact that the retrograde labelling observed in the posterior cingulate cortex in our study was localized to the more rostral

regions, which are suggested to have somatomotor functions as they also project to area 4γ (Olson CR and I Jeffers 1987; Olson CR and SY Musil 1992b; Musil SY and CR Olson 1993).

While area 4δr is, by definition, a part of area 4, it is cytoarchitectonically distinct from area 4γ (M1) and should probably be considered as part of premotor cortex (Ghosh S 1997c). In agreement with this proposition, the intensities of microstimulation required to produce motor effects from area 4δr were generally higher than those required to evoke movements from area 4γ (see also Ghosh S 1997c). Perhaps most importantly, however, the results from the current study shows that most of the recorded cells had complex activity patterns during the gait modifications, as compared to the simpler patterns of discharge and the stricter relationships with localized muscles of a single limb, commonly associated with area 4γ (Vicario DS et al. 1980; Beloozerova IN and MG Sirota 1993; Drew T 1993; Yakovenko S and T Drew 2015).

A Premotor network responsible for planning and execution of gait modifications

In the Introduction we presented the planning processes that we propose are needed to successfully step over a moving obstacle, together with predictions of the types of cell discharge patterns that would accompany those processes (Fig. 1). As summarized in Fig. 14 our results are generally compatible with our predictions and suggest the existence of a temporal progression of activity, from global signaling (primarily in area 6iffu) to more muscle-based signaling (primarily in area 4δr).

In the first place, we propose that the step-advanced, limb-independent cells (Fig. 14A) encode a global parameter relevant to the task, such as distance-to-contact, or estimated time-to-contact, as we have previously found in the PPC (Marigold DM and T Drew 2017, see below). This proposal is supported by the fact that many of the cells in PMC responded to looming visual stimuli outside the task. However, as in the PPC, not all step-advanced, limb-independent cells responded to looming and only 1 cell discharged earlier than 5 steps prior to the step over the obstacle, even though the obstacle was visible to the cat several steps prior to that. It is unlikely, therefore, that the cells are simply discharging to a visual stimulus. Rather, as in the PPC, we suggest that the discharge should be viewed more as contributing to a visuomotor transformation, or as part of a motor plan. In this respect, as we have previously noted (Andujar J-E *et al.* 2010), the modifications of gait required to step on a given target, as for example as in long-jumping (Lee DN et al. 1977; Lee DN et al. 1982), generally begin ~ 3 steps prior to take-off. We propose similarly that the changes in cell discharge observed in this study reflect the imminent need to adapt the gait to permit negotiation of the advancing obstacle. Such cells might alternatively, or complementarily, provide information on obstacle dimension, which is also a global variable that should be encoded in a limb-independent manner. However, the fact that only a few cells showed size-selectivity suggests that, at best, this is only a minor function of this population, or at least is not evident at the single-cell level in our task conditions.

Second, we suggest that there is a distributed population of step-advanced, limb-dependent cells that contributes to a competitive process of selection of the limb that will be the first to step over the obstacle. The cells in this population show a differential discharge in the left and right lead conditions and fall into 2 groups. In one of these groups (Fig 14B), cell discharge is related to the onset of the step over the obstacle in one condition but to the placement of the plant limb in the other condition. As such, the cell maintains a relationship to a given limb (more frequently the contralateral limb) in both conditions, similar to the prediction made in Fig. 1. In the other group

(Fig. 14C), cells discharge up to the onset of the step over the obstacle during both conditions but discharge during the step over the obstacle in only one of these conditions (generally the step over the obstacle by the contralateral limb). Such limb-dependent activity is reminiscent of that observed in primates prior to movement when they are given two possible targets to which to reach (Cisek P and JF Kalaska 2005). However, whether the discharge in our limb-dependent cells is actively involved in selecting the limb that will step over the obstacle or rather expresses a decision process that occurs elsewhere is not clear. Either possibility is compatible with our previous suggestion that limb selection is an emergent property dependent on the relationship of the obstacle to the body and current limb state (Marigold DM and T Drew 2017).

Complementary to these step-advanced, limb-dependent cells, are the step-related cells, both with and without rhythmical activity, that discharge during the step over the obstacle and/or in relationship to the plant limb. Indeed, the relative frequency of cells discharging in relation to the plant (left, contralateral) limb during the right lead condition (Fig. 14D-E) suggests that control of this behavioral event is as important a function of the PMC as the step over the obstacle itself. This is compatible with our previous finding that the inability to successfully negotiate an obstacle following lesion of the PPC results from inappropriate placement of the plant limb (Lajoie K and T Drew 2007). Moreover, the fact that cells related to the plant limb are found among all populations, including step-advanced, limb-independent cells (Fig. 5E) further suggests that determining the placement of the plant limb is an integral part of the planning process and is determined in concert with the activity of the limb that will pass over the obstacle.

However, in contrast to our prediction (Fig. 1C, *bottom*), we found only a few cells that showed step-by-step changes in activity occurring two or more steps before the step over the obstacle, including those in which modulation was superimposed on sustained activity preceding the step over the obstacle (see Fig. 7D). This is possibly because such changes are subtle and variable from one trial to another so that they will tend to be averaged out. Alternatively, it is possible that the implementation of such changes is expressed in the motor cortex where cells showing brief changes in activity in the steps preceding the obstacle were more frequently observed (Fig. S2E).

Lastly, although we have placed the emphasis on cells discharging in advance of, and with respect to, the lead forelimb, we also found evidence of cells that could contribute to interlimb coordination. This includes cells that are related to coupling between the two forelimbs (e.g. Fig. 8) and others that are related to coupling of the forelimb and hindlimbs (Fig. 9). Moreover, the fact that many of these cells only showed such activity during the gait modifications suggest that these cells in the PMC are implicated only in situations in which the normal coupling between limbs must be modified based on visual information. Some of these latter cells are similar to those that we have previously described in the PPC (Lajoie K et al. 2010) although others differ in showing changes in activity prior to the step over the obstacle by the forelimb. Last, and in a similar context, it is possible that the small subset of forelimb-hindlimb cells that we previously described in the fundus of the more lateral regions of the cruciate sulcus (Widajewicz W *et al.* 1994) were in fact located in 4δr and not area 4γ.

Taken together, the range of neuronal discharge patterns observed in the ventral bank of the PMC suggests that the network of cells in this region provides a complete substrate for transforming information about an approaching obstacle into the appropriate motor plan to allow an organism

to negotiate that obstacle. The fact that cells with different properties are intermingled suggests that, to some extent, this is a parallel process. However, the fact that rhythmical cells with complex properties are more frequent in area 4δr suggests that there is also a serial process in which information passes from more medial parts of the ventral bank to the more lateral parts, ending within primary MI where most cells show step-related discharge related only to activity in the contralateral limb (Fig. 14F and S2). Such a medio-lateral gradient would agree with the anatomical findings of Olson (Olson CR and I Jeffers 1987) who suggested the existence of a gradient in which the more medial regions of 6iffu are involved in visual processing and more lateral regions become progressively more somatomotor. This gradient could contribute to the transformation of global information into muscle-based outputs and would be facilitated by the strong projections between cells within area 6iffu. Further, the presence of inputs from cingulate and prefrontal cortex (Olson CR and I Jeffers 1987) suggest that activity in area 6iffu could be particularly involved in context-dependent planning of the gait modifications and might possibly contribute to spatial memory (Musil SY and CR Olson 1993).

Premotor cortex as part of a cortical Network: Comparison with the PPC and M1.

Planning a complex activity, such as a visually-guided gait modification, undoubtedly involves the contribution of a large network of cortical and subcortical structures (Drew T and DS Marigold 2015). To date, we only have detailed information on one other cortical structure involved in planning gait modifications, the PPC (Beloozerova IN and MG Sirota 2003; Andujar J-E *et al.* 2010; Lajoie K *et al.* 2010; Marigold DM and T Drew 2017), together with some evidence of the contribution of the cerebellum to visually-guided locomotion (Marple-Horvat DE and JM Criado 1999; Cerminara NL et al. 2005; Aoki S et al. 2013) and some fragmentary evidence for the contribution of the basal ganglia (Perrot O et al. 2009).

One of the hallmarks of cells involved in planning is that their activity must change in advance of the motor activity resulting from that process. In this respect, many cells within both the PPC and the PMC show this characteristic. Given the projection from area 5b to area 6iffu (Fig. 12, see also Fig. 15), it is tempting to suggest that the step-advanced activity observed in area 6iffu might depend on input from regions of the PPC showing similar activity (Andujar J-E *et al.* 2010; Lajoie K *et al.* 2010; Marigold DM and T Drew 2017). However, the relatively weak nature of this projection and the finding that cells in area 6iffu discharge relatively earlier than those in area 5b (Fig. 11) suggest that this is unlikely. Instead, the timing data would suggest that the step-advanced cells in areas 6iffu might provide an input to the PPC, although anatomical support for this projection is missing. Alternatively, cells in areas 6iffu and area 5b, which both receive input from area 7 (see Fig. 15), might act in parallel to provide information important for planning the motor activity to different subregions of area 4, including MI. PPC would provide information on the relative location of the object with respect to the body (Marigold DM and T Drew 2017) while area 6iffu might provide context-dependent information and be more directly involved in transforming global information to specific motor commands via its projections to 4δr (Ghosh S 1997a, 1997d) and, to a lesser extent, to area 4γ (Ghosh S 1997a; Andujar J-E and T Drew 2007). However, while signals compatible with limb selection (*see* Fig. 14B) were observed in area 6iffu, no such cells were found in PPC, compatible with our previous suggestion that limb selection occurs downstream of the PPC, perhaps in subcortical structures, and on the basis of integration of obstacle location with body state (Marigold DM and T Drew 2017).

Condition-selectivity of the step-related cells in the PPC and M1 showed both similarities and differences with respect to that observed in the step-related cells within the PMC. The major similarity was clearly the finding that cells in all three populations preferentially discharged as the left limb stepped over the obstacle in the left lead condition, suggesting a common role in the regulation of the contralateral limb in this situation. However, there was a clear tendency for the cells in M1 to discharge in much shorter bursts of activity than either those of the PPC or of the PMC. This would be compatible with our previous suggestions that the M1 population contributes to the regulation of specific synergistic groups of muscles active at different times before and during the step over the obstacle. The periods of activity preceding the step over the obstacle (Fig. S2E, F) might speak to an additional contribution of M1 to the step-by-step modulation of activity preceding the step over the obstacle, a characteristic that was largely absent in the PMC population (see above). This contribution of M1 to adapting gait prior to the step over the obstacle was not addressed in our previous studies, which concentrated primarily on the activity specifically related to the step over the obstacle. All 3 populations equally showed a contribution to the regulation of the contralateral limb in the right lead condition; however, in 2 very different manners. Most of the step-related cells in the PPC preferentially discharged as the left limb trailed the right limb over the obstacle, as did many of the cell in M1. In contrast, in the PMC, cells that showed significant changes in net activity in the right lead condition discharged preferentially with respect to the placement of the left limb in front of the obstacle (plant limb). Only a few such cells were found in the PPC population, although slightly more were observed in M1.

Comparison with the contribution of the PMC to planning activity during reaching movements in primates

Cytoarchitectonic area 6 in monkeys is an heterogeneous area that is divided into a number of subregions on the basis of connectivity and the functional characteristics of cell discharge (see Dum RP and PL Strick 2002 for review). The question then arises as to whether there are analogies between the cat and primate subregions. Some attempt has been made to answer this question on the basis of anatomical connections and microstimulation (Ghosh S 1997c, 1997a, 1997d) but the lack of information on the functional characteristics of the cells in different regions makes a fuller comparison problematic.

On the basis of our results, we propose that from both an anatomical and functional viewpoint, area 6iffu may be an analogue of the pre-SMA in the monkey (see Fig. 15). As for area 6iffu (see above), pre-SMA in the primate receives strong inputs from the cingulate (Luppino G *et al.* 1993) and the prefrontal cortex (Luppino G *et al.* 1993; Lu M-T et al. 1994). As for 6iffu (Ghosh S 1997c, 1997a; Andujar J-E and T Drew 2007), pre-SMA does not have strong projections to MI and does not project to the spinal cord (Dum RP and PL Strick 1992; Luppino G *et al.* 1993;Luppino G et al. 1994). In addition, limb responses as a result of microstimulation are absent or difficult to evoke from both 6iffu (see also Ghosh S 1997c) and pre-SMA (Luppino G et al. 1991; Matsuzaka Y et al. 1992). More importantly, cells in pre-SMA have similar properties to those in area 6iffu. These include the presence of limb-, or effector-, independent cells that show prolonged discharges beginning during the delay period of an instructed task and continuing during movement (Rizzolatti G *et al.* 1990; Matsuzaka Y *et al.* 1992; Fujii N et al. 1998; Hoshi E and J Tanji 2004; Nakajima T et al. 2013) and the prevalence of responses to visual stimuli (Rizzolatti G *et al.* 1990; Matsuzaka Y *et al.* 1992). The pre-SMA in primates also contributes strongly to preparing a temporal sequence of activity for a future movement (Shima K and J Tanji 2000; Nakajima T et

al. 2009; Nakajima T *et al.* 2013). One might speculate that such a function is similar to the preparation of the step-by-step changes that occur prior to the step over the obstacle, again speaking to common principles of organization.

With respect to 4δr, it is possible that it is an analog of primate SMA, as also suggested by Ghosh (Ghosh S 1997a) (Fig. 15). First, the activity of the majority of neurons in this area was limb-dependent, similar to the arm-dependent activity reported in primate (Kermadi I et al. 1998; Hoshi E and J Tanji 2004; Nakajima T *et al.* 2013). Second, microstimulation frequently evoked movements, albeit with a higher intensity current than for MI, as is also the case in primate SMA (Macpherson JM et al. 1982; Luppino G *et al.* 1991). Third, neurons in this area responded to tactile stimuli applied to the contralateral forelimb, as for SMA neurons (Wiesendanger M et al. 1985). Fourth, this area has connections to the adjacent MI and has a direct projection to the spinal cord (Ghosh S 1997c), which is also the case for SMA (Dum RP and PL Strick 1991; Matsuzaka Y *et al.* 1992). Fifth, this area has denser connections to parietal area 5 than area 7 (Ghosh 1997a), as is also the case with primate SMA (Luppino G *et al.* 1993). Further, this area has few neurons that respond to visual stimuli, unlike those in other area 6 regions in the primate, e.g. PMd, PMv, which are rich in neurons with visual responses (Boussaoud D et al. 1993; Crammond DJ and JF Kalaska 1994; Gallese V et al. 1996; Graziano MSA et al. 1997; Hoshi E and J Tanji 2006). Last, it is pertinent that the transfer of information that we propose occurs between 6iffu and area 4δr is very similar to that described between the pre-SMA and the SMA in the primate (Hoshi E and J Tanji 2004).

While the discharge patterns of the cells that we recorded are consistent with those obtained in primates, it must be remembered that the task conditions in the experiments that are being compared are quite different. Most experiments in primates are performed in subjects that are restrained and making movements towards an object that is fixed in space. In contrast, in our experiments, there is relative movement between the subject (the walking cat) and the target (the advancing target). This introduces several constraints that are unique to locomotion, as we introduced in Fig. 1. Thus, while in both primate pre-SMA and in areas 6iffu (and in the PPC) cells discharge to visual stimuli in advance of the movement, in our experimental situation we propose that the discharge extracts information about the advance of the obstacle and must be used dynamically to adjust gait prior to the execution of the step over the obstacle. Similar properties have been described by Graziano in both PPC and in ventral PMC in response to objects moved towards the face (Graziano MS and DF Cooke 2006) and equally observed in pre-SMA (Rizzolatti G *et al.* 1990). Similarly, our task requires selection of which limb will be the first to step over the obstacle. In our conditions we have proposed (Marigold DM and T Drew 2017) that this is an emergent process determined by the integration of a signal concerning information about gap closure and a signal containing information about limb state (on each side of the body). This process would presumably select the plant limb and regulate its activity. Analogous task-conditions do not frequently occur in most reaching tasks but, of course, would occur during primate locomotion, providing an opportunity to determine the similarities in structure and function between species. Once the first limb to step over the obstacle is selected, it is likely that the determination of movement-related discharges in structures such as the SMA (and PMd) would be the same in both motor activities, as it is in the motor cortex (Yakovenko S and T Drew 2015).

Conclusions

Together the physiological and anatomical data presented in this report strongly support a view that cortical subregions within the ventral bank of the cruciate sulcus make an important contribution to the planning of visually-guided gait modifications. Moreover, we present evidence to suggest not only that both cortical regions that we examined should be considered as parts of a complex and functionally-segregated premotor cortex within the cat cruciate sulcus, but that these regions may well be analogous to specific regions of the much better-defined primate premotor cortex. From a functional viewpoint, the results are important in describing the properties of a rich network of premotor cells that we propose contribute to different aspects of the planning processes required to negotiate a complex environment, including: object location, limb-selection, step-by-step modulation of activity during the approach to the obstacle, accurate placement of the plant limb and the initiation of the step over the obstacle. Together, we propose that this information determines the timing and the magnitude of the synergistic patterns of muscle activity (Krouchev N and T Drew 2013; Drew T and DS Marigold 2015) that are required to negotiate an obstacle.

Acknowledgements

We would like to thank T. Ariel, M. Bourdeau, N. De Sylva, P. Drapeau, F. Lebel and J. Soucy for technical assistance in the performance and analysis of these experiments. We also thank Nabiha Yahiaoui who participated in some of these experiments. We thank Drs. Elaine Chapman and Paul Cisek for helpful comments on this manuscript. We also extend our thanks to Dr. Kaoru Takakusaki for his help. This work was supported by an operating grant (PJT-156281) from the CIHR.

Reference List

Andujar J-E, Drew T. 2007. Organization of the projections from the posterior parietal cortex to the rostral and caudal motor cortex of the cat. J Comp Neurol. 504:17-41.

Andujar J-E, Lajoie K, Drew T. 2010. A contribution of area 5 of the posterior parietal cortex to the planning of visually guided locomotion: limb-specific and limb-independent effects. J Neurophysiol. 103:986-1006.

Aoki S, Sato Y, Yanagihara D. 2013. Lesion in the lateral cerebellum specifically produces overshooting of the toe trajectory in leading forelimb during obstacle avoidance in the rat. J Neurophysiol. 110:1511-1524.

Avendaño C, Isla AJ, Rausell E. 1992. Area 3a in the cat. II. Projections to the motor cortex and their relations to other corticocortical connections. J Comp Neurol. 321:373-386.

Avendaño C, Rausell E, Perez-Aguilar D, Isorna S. 1988. Organization of the association cortical afferent connections of area 5: A retrograde tracer study in the cat. J Comp Neurol. 278:1-33.

Batschelet E. 1981. Circular statistics in biology. New York: Academic Press.

Beloozerova IN, Sirota MG. 1993. The role of the motor cortex in the control of accuracy of locomotor movements in the cat. J Physiol. 461:1-25.

Beloozerova IN, Sirota MG. 2003. Integration of motor and visual information in the parietal area 5 during locomotion. J Neurophysiol. 90:961-971.

Berrevoets CE, Kuypers HGJM. 1975. Pericruciate cortical neurons projecting to brain stem reticular formation , dorsal column nuclei and spinal cord in the cat. Neurosci Lett. 1:257-262.

Boussaoud D, Barth TM, Wise SP. 1993. Effects of gaze on apparent visual responses of frontal cortex neurons. Exp Brain Res. 93:423-434.

Brinkman C. 1984. Supplementary motor area of the monkey's cerebral cortex: short- and long-term deficits after unilateral ablation and the effects of subsequent callosal section. J Neurosci. 4:918-929.

Cerminara NL, Edge AL, Marple-Horvat DE, Apps R. 2005. The lateral cerebellum and visuomotor control. Prog Brain Res. 148:213-226.

Cisek P, Kalaska JF. 2005. Neural correlates of reaching decisions in dorsal premotor cortex: specification of multiple direction choices and final selection of action. Neuron. 45:801-814.

Crammond DJ, Kalaska JF. 1994. Modulation of preparatory neuronal activity in dorsal premotor cortex due to stimulus-response compatibility. J Neurophysiol. 71:1281-1284.

Crammond DJ, Kalaska JF. 2000. Prior information in motor and premotor cortex: Activity during the delay period and effect on pre-movement activity. J Neurophysiol. 84:986-1005.

Drew T. 1988. Motor cortical cell discharge during voluntary gait modification. Brain Res. 457:181-187.

Drew T. 1993. Motor cortical activity during voluntary gait modifications in the cat. I. Cells related to the forelimbs. J Neurophysiol. 70:179-199.

Drew T, Andujar J-E, Lajoie K, Yakovenko S. 2008. Cortical mechanisms involved in visuomotor coordination during precision walking. Brain Res Rev. 57:199-211.

Drew T, Doucet S. 1991. Application of circular statistics to the study of neuronal discharge during locomotion. J Neurosci Methods. 38:171-181.

Drew T, Dubuc R, Rossignol S. 1986. Discharge patterns of reticulospinal and other reticular neurons in chronic, unrestrained cats walking on a treadmill. J Neurophysiol. 55:375-401.

Drew T, Marigold DS. 2015. Taking the next step: cortical contributions to the control of locomotion. Curr Opin Neurobiol. 33:25-33.

Dum RP, Strick PL. 1991. The origin of corticospinal projections from the premotor areas in the frontal lobe. J Neurosci. 11:667-689.

Dum RP, Strick PL. 1992. Medial wall motor areas and skeletomotor control. Curr Opin Neurobiol. 2:836-839.

Dum RP, Strick PL. 2002. Motor areas in the frontal lobe of the primate. Physiology & Behavior. 77:677-682.

Fogassi L, Gallese V, Buccino G, Craighero L, Fadiga L, Rizzolatti G. 2001. Cortical mechanism for the visual guidance of hand grasping movements in the monkey: A reversible inactivation study. Brain. 124:571-586.

Foster JD, Nuyujukian P, Freifeld O, Gao H, Walker R, S IR, T HM, Murmann B, M JB, Shenoy KV. 2014. A freely-moving monkey treadmill model. J Neural Eng. 11:046020.

Friel KM, Drew T, Martin JH. 2007. Differential activity-dependent development of corticospinal control of movement and final limb position during visually-guided locomotion. J Neurophysiol. 97:3396 - 3406.

Fujii N, Mushiake H, Tanji J. 1998. An oculomotor representation area within the ventral premotor cortex. Proc Natl Acad Sci. 95:12034-12037.

Fukuyama H, Ouchi Y, Matsuzaki S, Nagahama Y, Yamauchi H, Ogawa M, Kimura J, Shibasaki H. 1997. Brain functional activity during gait in normal subjects: a SPECT study. Neurosci Lett. 228:183-186.

Gallese V, Fadiga L, Fogassi L, Rizzolatti G. 1996. Action recognition in the premotor cortex. Brain. 119:593-609.

Ghosh S. 1997a. Comparison of the cortical connections of areas 4gamma and 4d in the cat cerebral cortex. J Comp Neurol. 388:371-396.

Ghosh S. 1997b. Cytoarchitecture of sensorimotor areas in the cat cerebral cortex. J Comp Neurol. 388:354-370.

Ghosh S. 1997c. Identification of motor areas of the cat cerebral cortex based on studies of cortical stimulation and corticospinal connections. J Comp Neurol. 380:191-214.

Ghosh S. 1997d. Ipsilateral cortical connections of area 6 in the cat cerebral cortex. J Comp Neurol. 388:397-414.

Graziano M. 2006. The organization of behavioral repertoire in motor cortex. Annu Rev Neurosci. 29:105-134.

Graziano MS, Cooke DF. 2006. Parieto-frontal interactions, personal space, and defensive behavior. Neuropsychologia. 44:845-859.

Graziano MSA, Hu XTA, Gross CG. 1997. Visuospatial properties of ventral premotor cortex. J Neurophysiol. 77:2268-2292.

Grillner S, Wallen P. 1985. Central pattern generators for locomotion,with special reference to vertebrates. Ann Rev Neurosci. 8:233-261.

Guitton D, Mandl G. 1978. Frontal oculomotor area in alert cat. I. Eye movements and neck activity evoked by stimulation. Brain Res. 149:295-312.

Hanakawa T, Katsumi Y, Fukuyama H, Honda M, Hayashi T, Kimura J, Shibasaki H. 1999. Mechanisms underlying gait disturbance in parkinson's disease. A single photon emission computed tomography study. Brain. 122:1271-1282.

Hassler R, Muhs-Clement K. 1964. Architektonischer aufbau des sensomotorischen und parietalen cortex der katze. J Hirnforsch. 6:377-420.

Hoshi E, Tanji J. 2000. Integration of target and body-part information in the premotor cortex when planning action. Nature. 408:466-470.

Hoshi E, Tanji J. 2004. Differential roles of neuronal activity in the supplementary and presupplementary motor areas: From information retreival to motor planning and execution. J Neurophysiol. 92:3499.

Hoshi E, Tanji J. 2006. Differential Involvement of Neurons in the Dorsal and Ventral Premotor Cortex During Processing of Visual Signals for Action Planning. J Neurophysiol. 95:3596-3616.

Jiang W, Drew T. 1996. Effects of bilateral lesions of the dorsolateral funiculi and dorsal columns at the level of the low thoracic spinal cord on the control of locomotion in the adult cat .1. Treadmill walking. J Neurophysiol. 76:849-866.

Kakei S, Hoffman DS, Strick PL. 2001. Direction of action is represented in the ventral premotor cortex. Nat Neurosci. 4:1020-1025.

Kermadi I, Liu Y, Tempini A, Calciati E, Rouiller EM. 1998. Neuronal activity in the primate supplementary motor area and the primary motor cortex in relation to spatio-temporal bimanual coordination. Somatosens Mot Res. 15:287-308.

Krouchev N, Drew T. 2013. Motor cortical regulation of sparse synergies provides a framework for the flexible control of precision walking. Front Comp Neurosci. 7.

Kurata K, Hoffman DS. 1994. Differential effects of muscimol microinjection into dorsal and ventral aspects of the premotor cortex of monkeys. J Neurophysiol. 71:1151-1164.

Lajoie K, Andujar J-E, Pearson KG, Drew T. 2010. Neurons in area 5 of the posterior parietal cortex in the cat contribute to interlimb coordination during visually guided locomotion: a role in working memory. J Neurophysiol. 103:2234-2254.

Lajoie K, Drew T. 2007. Lesions of area 5 of the of the posterior parietal cortex in the cat produce errors in the accuracy of paw placement during visually guided locomotion. J Neurophysiol. 97:2339-2354.

Lavoie S, Drew T. 2002. Discharge characteristics of neurons in the red nucleus during voluntary gait modifications: a comparison with the motor cortex. J Neurophysiol. 88:1791-1814.

Lee DN, Lishman J, R., Thomson DB. 1982. Regulation of gait in long jumping. J Exp Psychol Hum Percept Perform. 8:448-459.

Lee DN, Lishman J, R., Thomson J. 1977. Visual guidance in the long jump. Athletics Coach. 11:26-30.

Lipski J. 1981. Antidromic activation of neurones as a analytical tool in the study of the central nervous system. J Neurosci Meth. 4:1-32.

Lu M-T, Preston JB, Strick PL. 1994. Interconnections between the prefrontal cortex and the premotor areas in the frontal lobe. J Comp Neurol. 341:375-392.

Luppino G, Matelli M, Camarda R, Rizzolatti G. 1993. Corticocortical connections of area F3 (SMA-proper) and area F6 (pre-SMA) in the macaque monkey. J Comp Neurol. 338:114-140.

Luppino G, Matelli M, Camarda R, Rizzolatti G. 1994. Corticospinal projections from mesial frontal and cingulate areas in the monkey. Neuroreport. 5:2545-2548.

Luppino G, Matelli M, Camarda RM, Gallese V, Rizzolatti G. 1991. Multiple representations of body movements in mesial area 6 and the adjacent cingulate cortex: an intracortical microstimulation study in the macaque monkey. J Comp Neurol. 311:463-482.

Macpherson JM, Marangoz C, Miles TS, WiesendangerM. 1982. Microstimulation of the supplementary motor area (SMA) in the awake monkey. Exp Brain Res. 45:410-416.

Malouin F, Richards CL, Jackson PL, Dumas F, Doyon J. 2003. Brain activations during motor imagery of locomotor-related tasks: a PET study. Hum Brain Mapp. 19:47-62.

Marigold DM, Drew T. 2017. Posterior parietal cortex estimates the relationship between object and body location during locomotion. Elife. Oct 20;6. pii: e28143. doi: 10.7554/eLife.28143.

Marigold DS, Andujar J-E, Lajoie K, Drew T. 2011. Motor planning of locomotor adaptations on the basis of vision: The role of the posterior parietal cortex. Prog Brain Res. 188:83-100.

Marigold DS, Drew T. 2011. Contribution of cells in the posterior parietal cortex to the planning of visually guided locomotion in the cat: effects of temporary visual interruption. J Neurophysiol. 105:2457-2470.

Marple-Horvat DE, Criado JM. 1999. Rhythmic neuronal activity in the lateral cerebellum of the cat during visually guided stepping. J Physiol. 518:595-603.

Matsuyama K, Drew T. 1997. The organization of the projections from the pericruciate cortex to the pontomedullary brainstem of the cat: a study using the anterograde tracer, Phaseolus vulgaris leucoagglutinin. J Comp Neurol. 389:617-641.

Matsuzaka Y, Aizawa H, Tanji J. 1992. A motor area rostral to the supplementary motor area (presupplementary motor area) in the monkey: Neuronal activity during a learned motor task. J Neurophysiol. 68:653-662.

McVea DA, Taylor AJ, Pearson KG. 2009. Long-lasting working memories of obstacles established by foreleg stepping in walking cats require area 5 of the posterior parietal cortex. J Neurosci. 29:9396-9404.

Moll L, Kuypers HG. 1977. Premotor cortical ablations in monkeys: contralateral changes in visually guided reaching behavior. Science. 198:317-319.

Muakassa KF, Strick PL. 1979. Frontal lobe inputs to primate motor cortex: evidence for four somatopically organised "premotor" areas. Brain Res. 177:176-182.

Musil SY, Olson CR. 1993. The role of cat cingulate cortex in sensorimotor integration. In: Neurobiology of cingulate cortex and limbic thalamus: a comprehensive handbook Boston: Birkhauser p 345-365.

Nakajima T, Fortier-Lebel N, Yahiaoui N, Drew T. Characteristics of neuronal activity in putative premotor cortical areas of the cat during visually-guided locomotion. Society for Neuroscience; 2015; Chicago. 427.405/U417 p.

Nakajima T, Hosaka R, Mushiake H, Tanji J. 2009. Covert Representation of Second-Next Movement in the Pre-Supplementary Motor Area of Monkeys. J Neurophysiol. 101:1883-1889.

Nakajima T, Hosaka R, Tsuda I, Tanji J, Mushiake H. 2013. Two-Dimensional Representation of Action and Arm-Use Sequences in the Presupplementary and Supplementary Motor Areas. J Neurosci. 33:15533-15544.

Olson CR, Jeffers I. 1987. Organization of cortical and subcortical projections to area 6m of the cat. J Comp Neurol. 266:73-94.

Olson CR, Lawler K. 1987. Cortical and subcortical afferent connections of a posterior division of feline area 7 (area 7p). J Comp Neurol. 259:13-30.

Olson CR, Musil SY. 1992a. Posterior cingulate cortex:Sensory and oculomotor properties of single neurons in behaving cat. Cereb Cortex. 2:485-502.

Olson CR, Musil SY. 1992b. Topographic organization of cortical and subcortical projections to posterior cingulate cortex in the cat: Evidence for somatic, ocular, and complex subregions. J Comp Neurol. 324:237-260.

Palmer CI. 1978. A microwire technique for recording single neurons in unrestrained animals. Brain Res Bull. 3:285-289.

Perrot O, Laroche D, Pozzo T, Marie C. 2009. Quantitative assessment of stereotyped and challenged locomotion after lesion of the striatum: a 3D kinematic study in rats. PloS One. 4:e7616.

Rho M-J, Cabana T, Drew T. 1997. The organization of the projections from the pericruciate cortex to the pontomedullary reticular formation of the cat: a quantitative retrograde tracing study. J Comp Neurol. 388:228-249.

Rizzolatti G, Gentilucci M, Camarda RM, Gallese V, Luppino G, Matelli M, Fogassi L. 1990. Neurons related to reaching-grasping arm movements in the rostral part of area 6 (area 6ab). Exp Brain Res. 82:337-350.

Rossignol S. 1996. Neural control of stereotypic limb movements. In: Handbook of physiology. Section 12. Regulation and integration of multiple systems 5 ed. American Physiological society p 173-216.

Sacheli LM, Zapparoli L, Preti M, De Santis C, Pelosi C, Ursino N, Zerbi A, Stucovitz E, Banfi G, Paulesu E. 2018. A functional limitation to the lower limbs affects the neural bases of motor imagery of gait. NeuroImage Clin. 20:177-187.

Shima K, Tanji J. 1998. Both Supplementary and Presupplementary Motor Areas Are Crucial for the Temporal Organization of Multiple Movements. J Neurophysiol. 80:3247-3260.

Shima K, Tanji J. 2000. Neuronal activity in the supplementary and presupplementary motor areas for temporal organization of multiple movements. J Neurophysiol. 84:2148-2160.

Shine JM, Matar E, Ward PB, Bolitho SJ, Gilat M, Pearson M, Naismith SL, Lewis SJ. 2013. Exploring the cortical and subcortical functional magnetic resonance imaging changes associated with freezing in Parkinson's disease. Brain. 136:1204-1215.

Tokuno H, Tanji J. 1993. Input organization of distal and proximal forelimb areas in the monkey primary motor cortex: A retrograde double labeling study. J Comp Neurol. 333:199-209.

Udo M, Kamei H, Matsukawa K, Tanaka K. 1982. Interlimb coordination in cat locomotion investigated with perturbation. II. Correlates in neuronal activity of Deiter's cells of decerebrate walking cats. Exp Brain Res. 46:438-447.

Vicario DS, Martin JH, Ghez C. 1983. Specialized subregions in the cat motor cortex: a single unit analysis in the behaving animal. Exp Brain Res. 51:351-367.

Wagner J, Solis-Escalante T, Scherer R, Neuper C, Muller-Putz G. 2014. It's how you get there: walking down a virtual alley activates premotor and parietal areas. Front Hum Neurosci. 8:93.

Widajewicz W, Kably B, Drew T. 1994. Motor cortical activity during voluntary gait modifications in the cat. II. Cells related to the hindlimbs. J Neurophysiol. 72:2070-2089.

Wiesendanger M, Hummelsheim H, Bianchetti M. 1985. Sensory input to the motor fields of the agranular frontal cortex: A comparison of the precentral, supplementary motor and premotor cortex. Behav Brain Res. 18:89-94.

Wise SP, Mauritz KH. 1985. Set-related neuronal activity in the premotor cortex of rhesus monkeys: effects of changes in motor set. Proc R Soc Lond B Biol Sci. 223:331-354.

Wong C, Pearson KG, Lomber SG. 2017. Contributions of Parietal Cortex to the Working Memory of an Obstacle Acquired Visually or Tactilely in the Locomoting Cat. Cereb Cortex.1-16.

Yakovenko S, Drew T. 2015. Similar Motor Cortical Control Mechanisms for Precise Limb Control during Reaching and Locomotion. J Neurosci. 35:14476-14490.

Table 1: Tracer injections into area 6iffu

Case	Tracer	Aliquots (µl)*	Total injecte	Laterali ty	Section s	Analys is	Labelle d cell	Average cell
PRE M4	TR	[0.2 + 0.2] +	0.8	2.5	15 (1.7 – 7.3	1/10	520	35
PRE M6	AF488	[0.2 + 0.2]	0.4	3.5	10 (1.6 - 8.0	1/12	314	31
PRE M7	TR	[0.2 + 0.2] +	0.8	2.6	27 (1.6 - 7.9	1/6	4566	169
	FB	[0.2]	0.2	3	27 (1.6 - 7.9	1/6	6764	251
PRE M8	FB	[0.3]	0.3	4.9	14 (1.5 – 7.8	1/12	13281	949

Five injections were localized within area 6iffu. Tracer: TR = Texas Red; AF488 = Alexa Fluor 488; FB= Fast Blue. Column headings: *Aliquots*, volume of tracer injected at each location within the region targeted. In some sites, injections were made at two different depths within area 6iffu, e.g. [0.2 + 0.2) and in 2 cases (Prem4, TR and Prem7, TR), two injections were made at adjacent sites within area 6iffu. *Total injected,* total volume injected in a single case. *Laterality*, calculated with respect to the medial wall of the hemisphere. *Sections analyzed*, the number of sections for which we counted cells. *Analysis (section ratio),* the ratio of sections analyzed to those available, thus1/6 indicates that every sixth section was analyzed with a separation of 240µm between the analyzed sections. *Labelled cell count*, the total number of cells counted in the cortical regions that we explored for each experiment.

Table II: Classification of task-related neurons in areas 6iffu and 4δr.

Task-Related Cells (N=136)								
Step-Advanced Cells (86)				Step-Related Cells (41)				Unclassified (9)
Limb-Independent (64)		Limb-Dependent (22)		Tonic (19)		Rhythmic (22)		
FL	HL	FL	HL	FL	HL	FL	HL	
48	16	22	0	18	1	14	8	

Classification of cells into the 4 major groups identified in the Results section of the paper. Unclassified cells were task-related but could not be readily classified into one of these 4 identified groups of cells. FL and HL indicate cells whose activity was best related to the step over the obstacle by the forelimbs or hindlimbs, respectively. Note that all of the step-advanced HL cells showed initial changes in activity prior to the step over the obstacle by the FL and several of the step-related cells showed changes in activity that began just after the passage of the FLs over the obstacle.

Figure Legends

Figure 1: A theoretical framework for planning and executing visually-guided gait modifications. A: The processes involved in planning a step over a moving obstacle range from identifying the obstacle and its location to the execution of the step over the obstacle by the lead limb (adapted from Marigold DS *et al.* 2011). Only the planning processes for the initial step by the forelimb are illustrated. The staggered representation of the stages involved in the planning process represents the likelihood that both parallel and serial planning of the different processes is involved. B,C,D: cartoons of representative cell discharge patterns for different cortical regions when either the left limb, contralateral to the recording site (*left* panel) or the right limb (*right* panel) is the first to step over an obstacle. B,D, show, respectively, typical patterns of activity recorded from the posterior parietal cortex (PPC) and the motor cortex (M1) in previous experiments (see references in Introduction). C: predictions of the neuronal discharge patterns that we would expect to record from the premotor cortex (PMC) if it is involved in different aspects of the transformation of information about obstacle location (provided by the PPC) to the motor activity required to execute the step over the obstacle (produced from M1). Such cells include those implicated in: selection of the lead limb; determination of the limb trajectory and EMG patterns (parameters) required to negotiate the obstacle; step-by-step adjustments of the gait during approach to the obstacle; and determination of the location and timing of the placement of the plant limb. In the latter case, cell activity will be related to the placement of the left limb in front of the obstacle preceding the step over the obstacle by the right limb. E: electromyographic (EMG) activity from the left and right forelimb flexor muscles (lF and rF, respectively) corresponding, respectively to the contralateral (co) and ipsilateral (i) limbs with respect to the recording site. Note that in this, and in all other figures, blue traces represent unobstructed locomotion, red traces indicate the left lead condition and green traces indicate the right lead condition. Dotted lines represent a change in activity related to a smaller obstacle (parameterization).

Figure 2: Method for quantitative analysis of cell discharge. A and B: *Top*, Peri-event histograms (PEHs) as calculated according to Udo's method (gray traces, see text)(Udo M et al. 1982) or from moving window averages (colored traces). Moving window averages (see text) show mean discharge frequency together with the confidence interval (CI = 0.05) of the standard error of the mean (SE) for the left lead (red trace in A) and right lead (green trace in B) conditions for the step over the obstacle and for 3 step cycles (6 steps) prior to that step and 1 step cycle (2 steps) after. These data are superimposed on the averaged activity during control steps (blue traces), displayed together with the interval of confidence ($p<0.05$: filled blue area). Note that for the control traces (blue traces), neuronal activity during each unobstructed step cycle is considered to be identical and cell activity from the 4^{th} step cycle before the step over the obstacle is repeated in each illustrated step cycle (see text). Windows where activity was significantly different from control ($p < 0.05$) are indicated with small, horizontally-oriented, bars under the PEHs (black bars indicate increased activity; gray bars, decreased activity). *Bottom:* raster plots of discharge activity together with the mean rectified EMG in the left and right brachialis (lBr and rBr, respectively). Numbers on the EMG traces indicate steps prior to or following the step over the obstacle (identified as step 0). Data in A are synchronized to the onset of the lBr and those in B to the rBr. The vertical lines indicate the onset of step cycles (onset of Br) and the staggered lines indicate the end of the period of Br activity; activity is rank-ordered according to the duration of the flexor muscle activity in each trial. The long, thick, vertical line indicates the onset of the step over the

obstacle. The shaded, vertically-oriented, rectangle superimposed on the PEH in A,B is equal to 0.4 of a step (see text). C,D: PEHs showing mean discharge frequency and CI in the left (C) and right (D) lead conditions during steps over the larger (C, red lines; D, green lines) and smaller (cyan lines) obstacle respectively. E: Distributions of firing rates for the analysis window indicated in A,B (vertical shaded bar) for the left lead (filled red circles) and right lead (filled green circles) conditions, and those for the matched windows in control steps (small blue squares and diamonds). The means and 95% confidence intervals for each condition and control are indicated with the larger symbol and error bars beside the small symbols. Given that the dummy value for the control is 0 and that for the steps over the obstacle is 1, the slopes of the lines correspond to the net activity in left-lead (red) and right-lead (green) conditions. F: Net activity (discharge activity during left or right lead condition – discharge activity in the unobstructed condition) in left-lead (red) and right-lead (green) conditions, together with 95% CI.

Figure 3: Histological reconstruction. A-C: location of all penetrations (circles) in P1 (A) and P2 (B, C) plotted on flattened representations of the peri-cruciate cortex and aligned to the fundus of the cruciate sulcus (0 mm). Thick black lines indicate the borders and fundi of sulci; small dotted lines differentiate cytoarchitectonic regions. A,B: cells classified as step-advanced in P1 and P2; C: cells classified as step-related (P2). Legends at the foot of A-C indicate the different classes of cells illustrated in each figure. D: Examples of individual penetrations into the ventral bank of the peri-cruciate cortex traced from the para-sagittal histological sections. The penetrations illustrate the location of the recordings from cells illustrated in Figs. 5, 7, 8 and 9 (see identification code above each illustration). The dotted line indicates layer V. Illustrated trajectories are indicated on the flattened representations by red, horizontal, dotted lines. Small ticks differentiate different cytoarchitectural boundaries with area 6iffu, or 4δr, being identified in each figurine. Abbreviations: Ans, fundus of the ansate sulcus; Cor, fundus of the coronal sulcus; Cru, fundus of the cruciate sulcus; dlPFC, dorsolateral prefrontal cortex; PrS, fundus of the presylvian sulcus; 3, cytoarchitectonic area 3; 4δc, 4δr, 4γ, 4fu, 4sfu, different cytoarchitectonic sub-areas of cytoarchitectonic area 4; 6aα, 6aβ, 6aγ, 6iffu, different sub-areas of cytoarchitectonic area 6.

Figure 4: Periods of task-related activity. A: The period of significantly modified activity for all 22 task-related cells recorded in cat P1, as calculated during the left lead condition. Values on the x-axis indicate steps prior, or subsequent, to the step over the obstacle (step 0) as indicated in Fig. 2A. Black bars indicate facilitation and grey bars, suppression. Cells are rank-ordered according to the time of the earliest significant change in activity. B: similar plot for all 114 cells recorded in P2 for the left lead condition. Note that several neurons (cells 100-114) did not show task-related activity in the left lead condition. C: percentage of cells that showed facilitation and suppression of their discharge during the approach to, and the step over, the obstacle in the two cats. Solid vertical line, step over obstacle by the left limb; dotted vertical line at -1, step preceding the step over the obstacle (by the plant limb).

Figure 5: Examples of step-advanced, limb-independent cells. A: limb-independent cell in which the change in cell discharge began several steps before the obstacle and continued during the step over the obstacle. *Top panel*: averaged activity in left lead condition synchronized to lClB. *Middle panel*: activity in right lead condition synchronized to rClB. *Bottom panel*: superimposition of the left and right lead conditions, illustrating the limb-independent nature of the discharge. In each panel we illustrate, from top to bottom, the averaged and filtered cell activity, the raster of

the cell activity and the averaged EMG activity from the lClB and rClB. Red traces indicate activity in the left lead condition, green traces in the right lead condition and blue traces during unobstructed locomotion. Numbers on the EMG traces indicate steps prior to the step over the obstacle (step 0). B-F: additional examples, synchronized to the respective lead limb during the left and right lead conditions (see text). All cells recorded from area 6iffu. Solid vertical line indicates the onset of the step over the obstacle by the lead limb in all cases. Abbreviations: co, contralateral (left) limb; i, ipsilateral (right) limb; N, number of trials.

Figure 6. Timing relationships of limb-independent cells. A: Period of task-related activity of all 64 step-advanced, limb-independent cells (P1 and P2) aligned with respect to the onset (*left*) or to the offset of the initial period of discharge (*right*) for the left lead condition. In cells in which there were two periods of discharge preceding the step over the obstacle (N=2), we used the second of the two bursts for the alignment on the offset of activity. B: Percentage of cells showing significantly increased (thicker black line) or significantly decreased (gray line) activity during left and right lead. C: phase relationship of the time of offset of cell activity in the right lead condition as a function of that during the left lead condition. Offsets and onsets are calculated as percentage of a step cycle but are expressed as steps (step cycle *2). Diagonal lines indicate the line of equivalence and deviation from that line by 1 step. Arrows and the letters A-F indicate the cells illustrated in Fig. 5. Green colored circles indicate cells in which discharge ended just before, during or after the step over the obstacle (as in Figs. 5A-D); cyan symbols indicate cells ceasing activity ~ 1 step prior to the step over the obstacle (e.g. during the plant limb, Fig. 5E) and the blue circle indicates the cell ceasing activity 1 step cycle prior to the step over the obstacle (Fig. 5F). Red and salmon-colored symbols indicate cells that discharged until the passage of the hindlimbs over the obstacle. Red circles indicate cells with a monotonic change in activity while the salmon-colored symbols indicate cells with an initial period of activity prior to the passage of the forelimb (as in Fig. 5D). D: similar plot for the phase of onset of the task-related activity. E,F: histograms showing the difference in timing between the left and right lead conditions for the end (E) and onset (F) of the period of the task-related activity. Abbreviations: lClB_off, offset of activity in the lClB during left lead; lClB_on, onset of activity (phase=0.0); rClB-1_off, offset of activity in the rClB in the step before the step over the obstacle; lSrt_off, end of period of activity in the sartorius as the left hindlimb steps over the obstacle; lSt_on, onset of activity in the semitendinosus as the left hindlimb steps over the obstacle.

Figure 7: Examples of step-advanced, limb-dependent cells. A: Example of a cell in which task-related activity during the left lead condition (*top panel*) ceased at the onset of the step over the obstacle. In contrast, during the right lead condition (*middle panel*), the change in cell activity ceased during the period of activity of the left, contralateral, limb, prior to the step over the obstacle by the right limb. *Bottom panel*: the activity in the left and right lead condition is superimposed. Organization of figure similar to that in Fig. 5. B-D: Three other examples of cells (see text). Downward-oriented arrows in D emphasize peaks of activity in left lead (red arrows) and right lead (green arrows) conditions. Cells A-B recorded in area 4δr and C-D in area 6iffu. E: timing relationships of those limb-dependent cells that showed task-related activity in both conditions, organized as in Fig 6C,D. *Left panel*: offset of the task-related activity; *right panel*: onset of task-related activity. Cyan circles, cells discharging with respect to the plant limb in one condition (as in A,B); green circles, cells that discharged until or during the step over the obstacle in both conditions (as in C,D). The blue circle represents a cell that discharged with respect to the passage

of the left forelimb in the left lead condition but to the end of the preceding step in the right lead condition. Line perpendicular to the line of equivalence indicates the offset of activity in the rClB-1 (as in Fig. 6C), corresponding to the placement of the plant limb in front of the obstacle.

Figure 8: Examples of step-related cells. A,B: 2 examples of cells that showed task-related discharge activity only during the step over the obstacle in the left lead condition (red traces). During unobstructed locomotion (blue traces), the cells were either weakly modulated (A) or inactive (B). C: Cell that discharged only during the left plant step before the step over the obstacle by the right forelimb in the right lead condition (green traces). D,E: two strongly rhythmically-active cells in which discharge activity was increased during the step over the obstacle with the left limb in the left lead condition (red trace) but in the step before the step over the obstacle by the right limb in the right lead condition (green trace) (i.e., as in part C). Cell D was recorded simultaneously with cell C. F: cell that discharged in the period between the passage of the left and right forelimb in the left lead condition but in the period between the passage of the right and left forelimb in the right lead condition. Activity in all plots is synchronized to the onset of activity in the lClB in both the left and right lead conditions. Arrows, 'L' and 'R', indicate the step over the obstacle in the left and right lead condition, respectively; 'LP' indicates the placing of the left, contralateral, limb (plant limb) during the right lead condition. Cells in A and C-F recorded in area 4δr, cell B recorded in area 6iffu.

Figure 9: Hindlimb-related Activity. A: *top panel*: Example of a cell that modified its discharge prior to the step over the obstacle by the lead forelimb and then showed a prolonged period of increased discharge during the subsequent step over the obstacle by the hindlimb. Data are shown superimposed for left and right lead conditions and are synchronized to the onset of activity in the lead forelimb. Vertical dotted line indicates the end of the passage of the four limbs over the obstacle. *Middle panel*, Activity in left lead condition with cell activity synchronized to the onset of the right, ipsilateral, sartorius (rSrt), a flexor of the hip active during the swing phase of the hindlimb. *Bottom panel*: Activity in the right lead condition with cell activity synchronized to the onset of the lSrt. First vertical dotted line in the *middle and bottom* panels indicates the onset of activity in the lead forelimb. The second vertical dotted line indicates the end of the passage of the hindlimbs over the obstacle. Numbers (1-4) indicate the order of the passage of the four limbs during the steps over the obstacle in all 3 panels. B: Cell that showed step-related activity during the passage of the right hindlimb over the obstacle. Top panel: Left lead condition, data synchronized to the lClB. Bottom panel: Left lead condition, data synchronized to the right semitendinosus (rSt), a flexor of the knee active at the onset of hindlimb swing. C: Cell that showed multiple periods of task-related activity, starting with the passage of the left forelimb over the obstacle and continuing until passage of the right hindlimb. Data aligned on activity in the lClB. Asterisks in A-C indicate the muscle used to synchronize the averages. All cells recorded in area 6iffu. Abbreviations: LFL, left forelimb; LHL, left hindlimb; RHL right hindlimb.

Figure 10: Condition-Selectivity: A: Rank-ordered task-related activity in the left lead condition for the 4 major populations of cells (i-iv) that we categorized in this study. (*Ai* repeated from Fig. 6A). B: examples of condition-selective changes in net activity in 4 representative cells during left and right lead as indicated in Methods and Fig. 2F. Each example represents a previously illustrated cell: Bi taken from Fig. 5A; Bii from Fig. 7C; Biii from Fig. 8B; Biv from Fig. 8D. Red and green horizontal bars below the traces indicate periods in which the traces showed significant

differences (condition-selectivity) between the net activity in the left and right lead conditions. Red bars indicate periods in which net activity was significantly greater in the left lead condition and green bars periods in which net activity was significantly greater in the right lead condition. C: periods of significantly different net activity for all cells in each group. Arrows indicate the cells illustrated in B. D: Percentage of cells in each group showing significant condition-selectivity at different times during the task. Solid vertical line indicates the step over the obstacle by the lead limb; dotted vertical line indicates the step preceding the step over the obstacle, corresponding to the placement of the plant limb in front of the advancing obstacle. Cell discharge in A is aligned to the activity of the lBr/ClB; activity in B-D is aligned to the onset of the activity in the lead Br/ClB.

Figure 11: Comparison with PPC cells. A: The period of activity of all 129 cells recorded from the PPC that showed task-related activity for the left lead condition taken from 2 previous databases (Andujar J-E et al. 2010; Marigold DM and T Drew 2017) and plotted as in Fig. 4 B,C: cumulative histograms for all cells recorded from the PMC and the PPC (B) and for only those cells defined as step-advanced (C). Probability values (p) indicate the results of the Kolmogorov-Smirnov test for distribution (see text). D-E: 2 cells recorded from the PPC demonstrating discharge related to the activity in the contralateral limb. Cell discharge is synchronized to the activity of the lBr for both the left and right lead conditions, as for Fig. 8. F.G:Condition-selectivity for the step-related PPC cells, displayed as in Fig. 10C,D. The inset in Fig. 11F illustrates the net activity of the cells shown in Fig. 11D,E for the left and right lead conditions, but aligned now to the activity in the lead Br. In this display, the increase in net activity during the right lead condition for the cell in D occurs relatively later than that during the left lead condition (because the left limb trails the right limb). For the cell in E, the increase in net activity in the right lead condition (green trace) arrives 1 step before the step over the obstacle with the right limb; i.e. it maintains the relationship between LP and R shown in Fig. 11E.

Figure 12: Cortical projections to area 6iffu. A-D: 4 representative parasagittal sections of the peri-cruciate cortex showing the location of retrogradely-labelled cells following injections of Texas Red (red circles) and Fast Blue (blue circles) into area 6iffu. Each circle represents the presence of at least 1 cell in each 200µm bin (see Methods). Colored ovoids on sections A,B indicate the site of injections and the red and blue dotted lines indicate exclusion zones in which no cells were counted as they overlapped the injection sites. Square boxes indicate the region shown in the photomicrographs of E,F. E,F: photomicrographs showing the injection sites of Texas Red and Fast Blue in area 6iffu of the cruciate sulcus. G: drawing of the dorsal surface of the brain from the cat used in this experiment showing the location from which sections A-D were taken.

Figure 13: Summary of density of retrogradely-labelled cells. A,B: all cells labelled in the pericruciate cortex and the surrounding regions following the injections of Texas Red and Fast Blue illustrated in Fig. 12. Each circle represents the presence of at least 1 cell in a 200µm bin. Data are illustrated in 2 panels. In the left panel, data are aligned with the fundus of the cruciate sulcus (Cru) while in the right panel they are aligned to the most rostral point of the splenial sulcus (Spl). Negative values in the left panel are ventral and rostral to Cru. Negative values for the cingulate cortex indicate cells that are caudal and ventral (CV) to Spl and positive values those that are caudal and dorsal (CD). C-D: Cells are grouped according to the number of cells in each 200µm bin with red indicating 81-100% of the mean +SD value (see Methods) and cyan, 1-20%

(see key). E-F: contour plots illustrate the regions of highest density of labelling (red indicates the densest labelling and blue indicates the least); each contour represents a 5% increment in density.

Figure 14: Summary of discharge patterns in areas 6iffu and 4δr. A-E: Activity of selected cells recorded from the PMC during left and right lead conditions, left and right panels respectively, to demonstrate the major different classes of cells that we propose are involved in planning the step over the obstacle by the lead forelimb. Cell discharge patterns are illustrated as moving window averages (see Fig. 2 and Methods). F: selected cell recorded from area 4γ of cat P2 to show typical activity related only to the execution of the step over the obstacle by the contralateral limb. G: EMG activity recorded from the Br. The red, vertical, bar in the left panel indicates the step over the obstacle by the lead, left, contralateral, limb. The second, longer green, vertical, bar in the right panel indicates the step over the obstacle by the lead, right, ipsilateral, limb. The shorter green, vertical, bar preceding this indicates the period in which the contralateral limb is placed on the support surface in the step preceding the step over the obstacle.

Figure 15: Schematic representation of some of the major connections between different structures in the cat and the primate. The figure emphasizes the inputs from the prefrontal, cingulate, and PPC (areas 5 and 7) to the different regions of the PMC discussed in this manuscript. (see text for further description and for references). Note that we have only shown the major connections referred to in the text.

Fig. S1. Methods used for alignment of cell data. Four different methods of illustrating cell activity. A-D, cell with weak rhythmic activity during unobstructed locomotion, same cell as illustrated in Fig. 2. E-H, cell recorded from the PPC (same cell as illustrated in Fig. 5A of Andujar J-E *et al*. 2010) that showed strong rhythmicity during unobstructed locomotion. A,E: Activity during the left lead condition, aligned to the onset of the EMG activity in the lBr. B,F: Activity in the right lead condition aligned to the rBr. C,G: activity from the left (red traces) and right (green traces) lead conditions superimposed together with the cell activity in the unobstructed condition (blue traces) and aligned to the activity in the lead Br. Note that because activity is synchronized to the lBr for the left lead condition and to the rBr for the right lead condition, activity in each Br is phase-shifted by 0.5 step cycle in the two conditions. D,H: The same conditions as in C,G, but now illustrated with the data aligned to the activity in the lBr for both the left and right lead conditions. As such, cell activity occurs at the same phase in all conditions. In this display the increase in activity in the rBr in the right lead condition precedes the activity of the lBr (as the left forelimb is the second forelimb to pass over the obstacle, the trail forelimb). Data in each panel are organized as in Figs. 2A,B.

Fig. S2. Condition selectivity of motor cortical cells. A,B and C, examples of 3 different, rhythmically-modulated, motor cortical units recorded from cats MC28 (A,B) and MC29 (C) and used in a previous study (Yakovenko S and T Drew 2015). All 3 cells showed increased activity at different times during the step over the obstacle in the left lead condition, together with more variable changes in discharge during the step over the obstacle in the right lead condition. D: changes in net activity for the 3 units, now synchronized on the lead limb, as in Figs 10 and 11. E: periods of modified activity during the left lead condition, organized as for Fig. 3A (5 units showed changes in activity only in the right lead condition). F: periods of significant condition selectivity of each motor cortical unit. G: percentage of cells showing greater change in absolute net activity during the left (red traces) or right (green traces) lead conditions. Note that because motor cortical units frequently show only brief periods of modified activity (e.g. Unit 3), we reduced our criterion for significance from 5 bins to 4 bins. In addition, as we only measured the period of activity of the coBr in these former experiments, activity in the right lead condition has been right-shifted by 0.5 step cycles to approximate synchronization on the iBr.

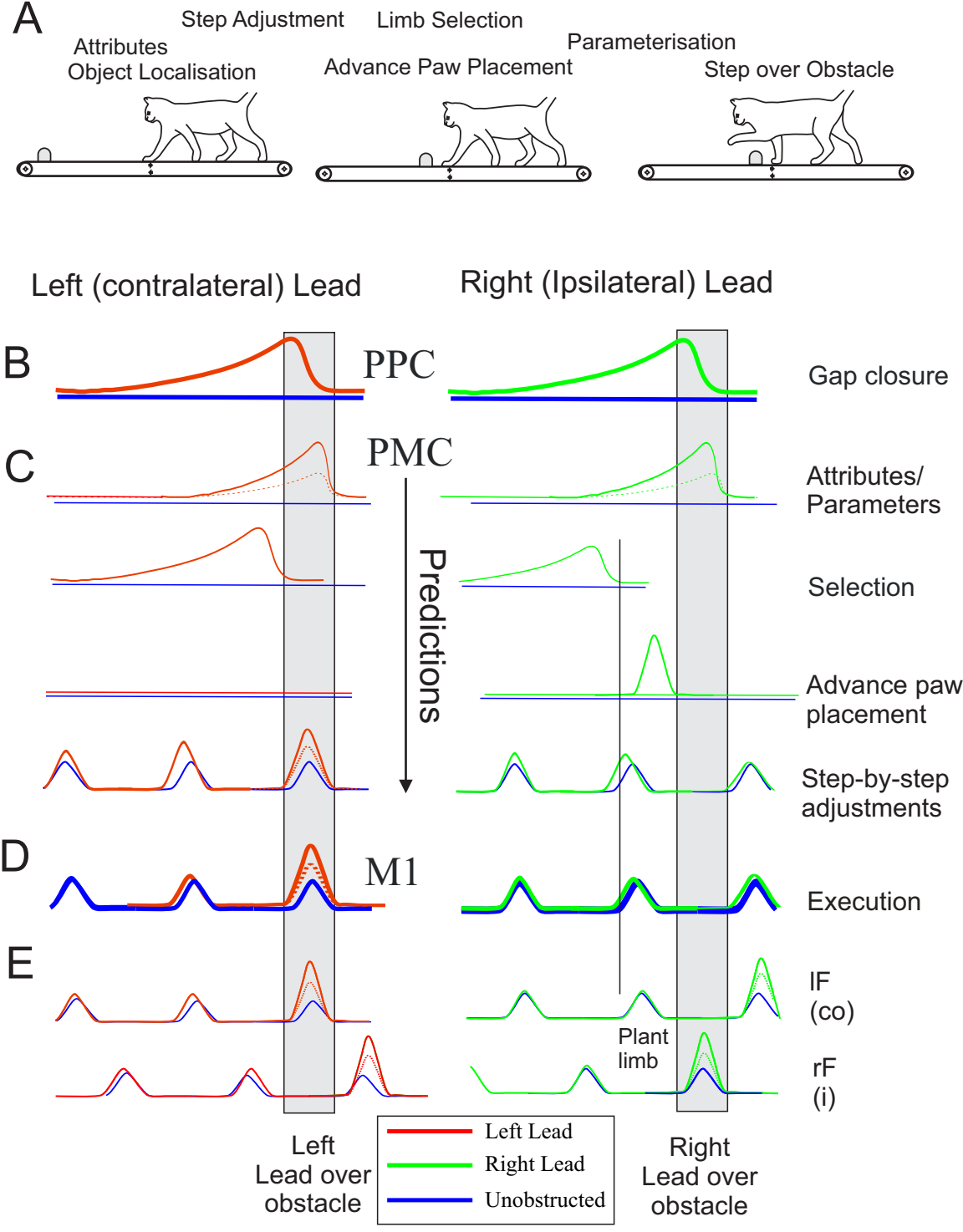
A
Step Adjustment
Limb Selection
Attributes
Object Localisation
Advance Paw Placement
Parameterisation
Step over Obstacle
Left (contralateral) Lead
Right (Ipsilateral) Lead
B
PPC
Gap closure
C
PMC
Attributes/
Parameters
Selection
Predictions
Advance paw
placement
Step-by-step
adjustments
D
M1
Execution
E
IF
(co)
Plant
limb
rF
(i)
Left
Lead over
obstacle
Left Lead
Right Lead
Unobstructed
Right
Lead over
obstacle

Fig. 1

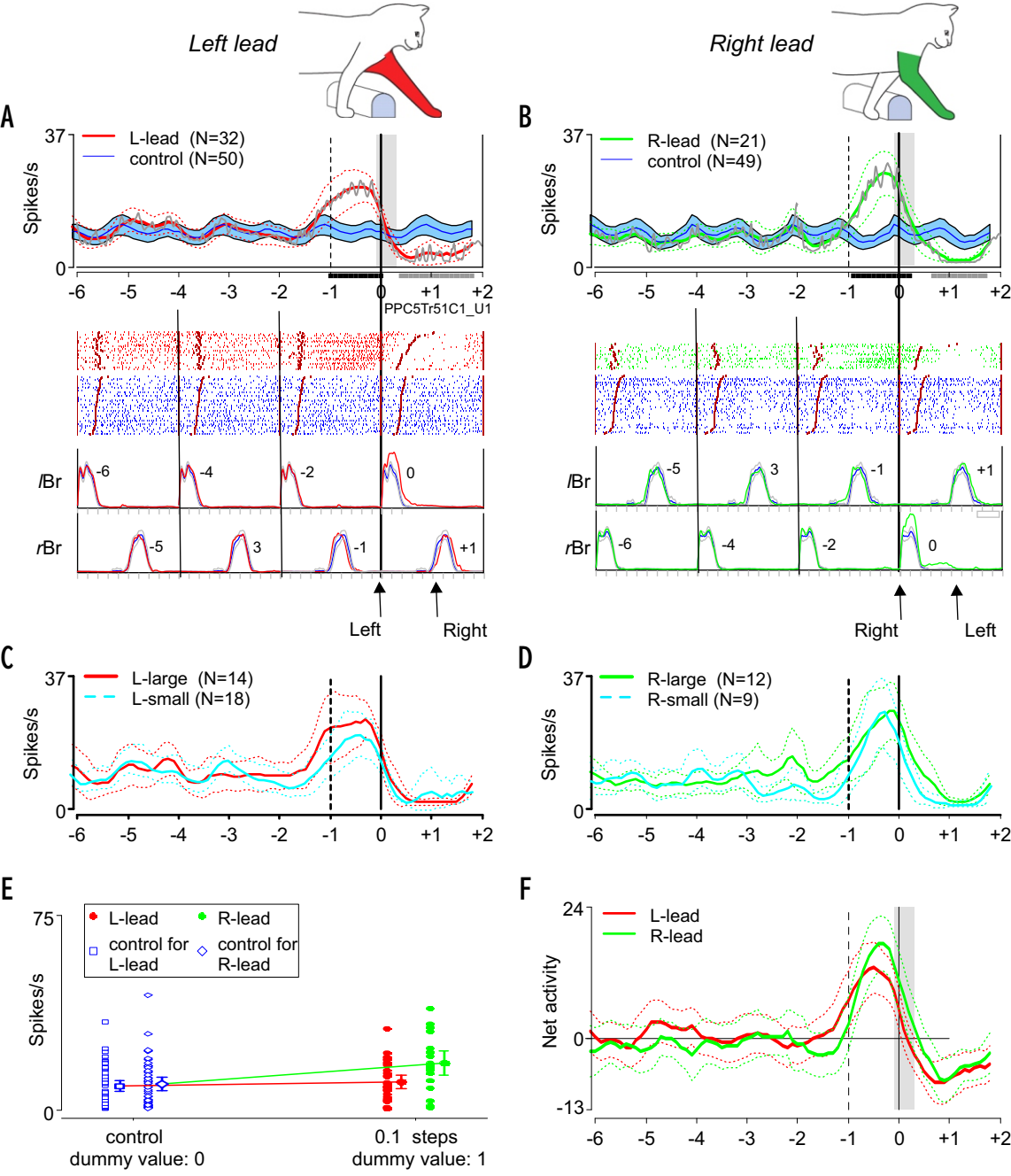
Left lead
Right lead
A
B
C
D
E
F
Spikes/s
37
0
L-lead (N=32)
control (N=50)
R-lead (N=21)
control (N=49)
-6 -5 -4 -3 -2 -1 0 +1 +2
PPC5Tr51C1_U1
lBr
rBr
-6 -4 -2 0
-5 3 -1 +1
-5 3 -1 +1
-6 -4 -2 0
Left
Right
Right
Left
L-large (N=14)
L-small (N=18)
R-large (N=12)
R-small (N=9)
75
L-lead
R-lead
control for L-lead
control for R-lead
control
dummy value: 0
0.1 steps
dummy value: 1
24
-13
Net activity
L-lead
R-lead

Fig. 2

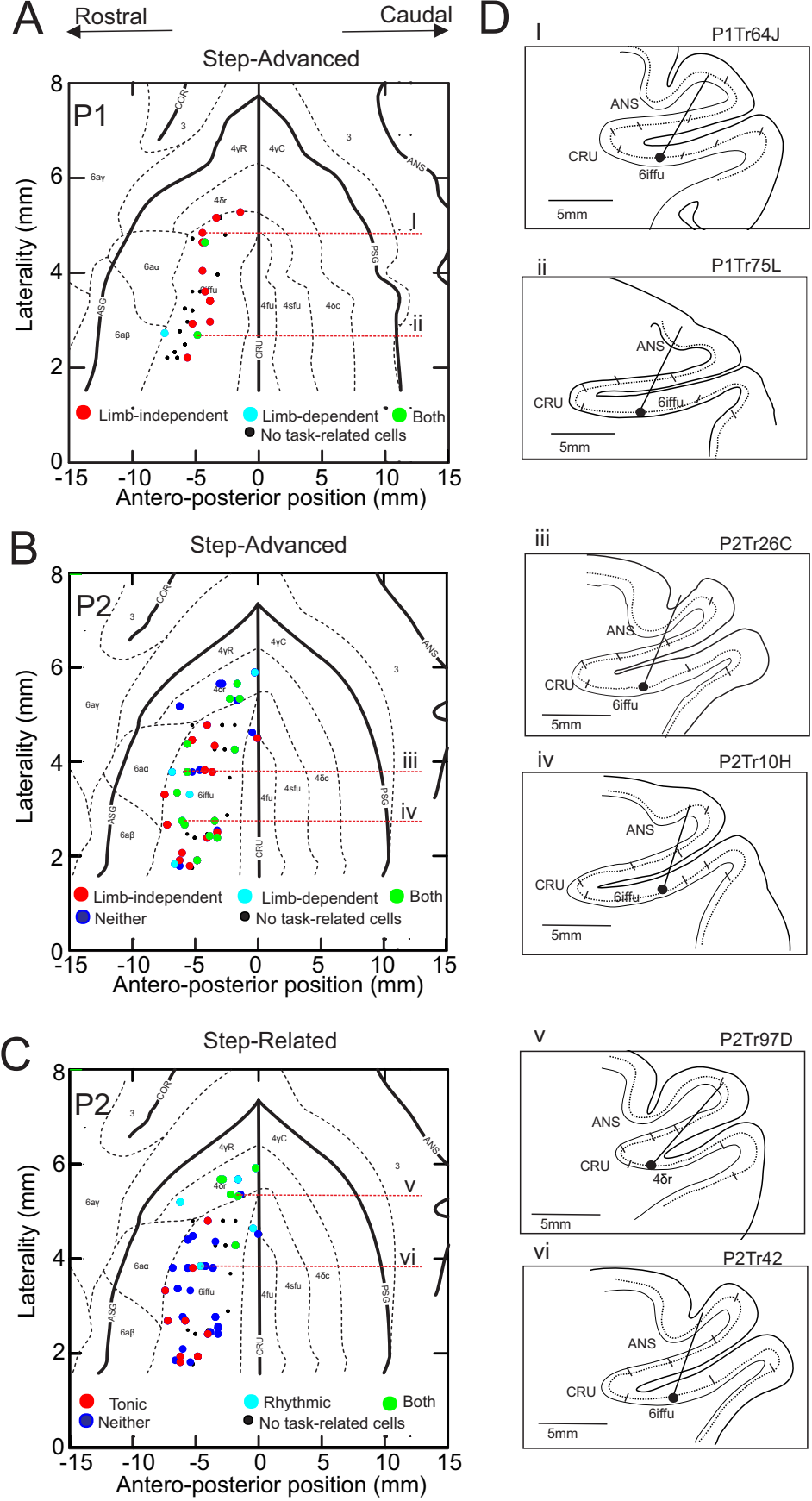
A
Rostral
Caudal
Step-Advanced
P1
Laterality (mm)
Antero-posterior position (mm)
Limb-independent
Limb-dependent
Both
No task-related cells
B
Step-Advanced
P2
Laterality (mm)
Antero-posterior position (mm)
Limb-independent
Limb-dependent
Both
Neither
No task-related cells
C
Step-Related
P2
Laterality (mm)
Antero-posterior position (mm)
Tonic
Rhythmic
Both
Neither
No task-related cells
D
i
P1Tr64J
ANS
CRU
6iffu
5mm
ii
P1Tr75L
ANS
CRU
6iffu
5mm
iii
P2Tr26C
ANS
CRU
6iffu
5mm
iv
P2Tr10H
ANS
CRU
6iffu
5mm
v
P2Tr97D
ANS
CRU
4δr
5mm
vi
P2Tr42
ANS
CRU
6iffu
5mm

Fig. 3

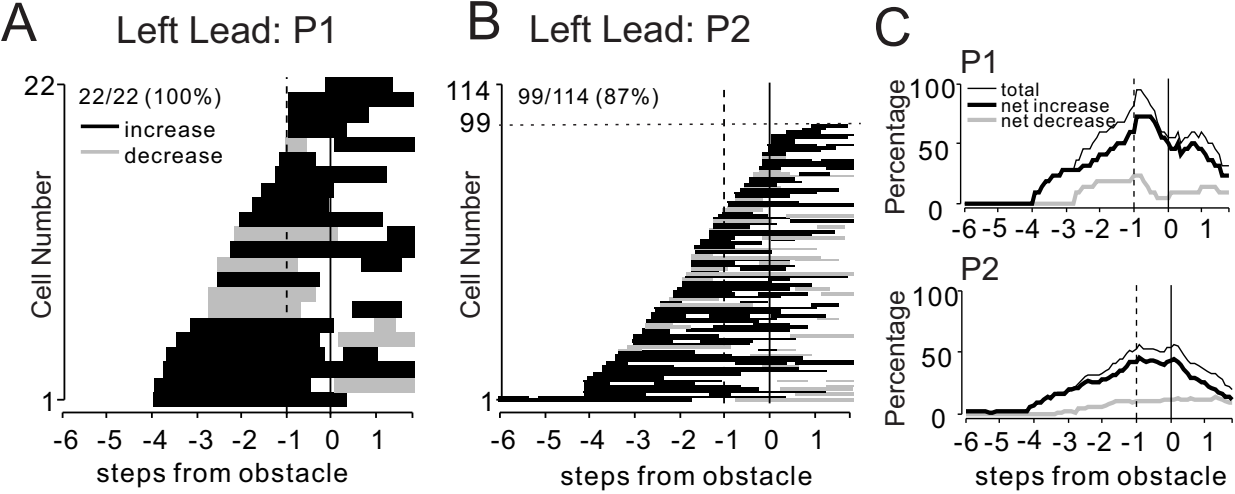
A
Left Lead: P1
22
22/22 (100%)
increase
decrease
Cell Number
1
-6 -5 -4 -3 -2 -1 0 1
steps from obstacle
B
Left Lead: P2
114
99
99/114 (87%)
Cell Number
1
-6 -5 -4 -3 -2 -1 0 1
steps from obstacle
C
P1
total
net increase
net decrease
Percentage
100
50
0
-6 -5 -4 -3 -2 -1 0 1
P2
Percentage
100
50
0
-6 -5 -4 -3 -2 -1 0 1
steps from obstacle

Fig. 4

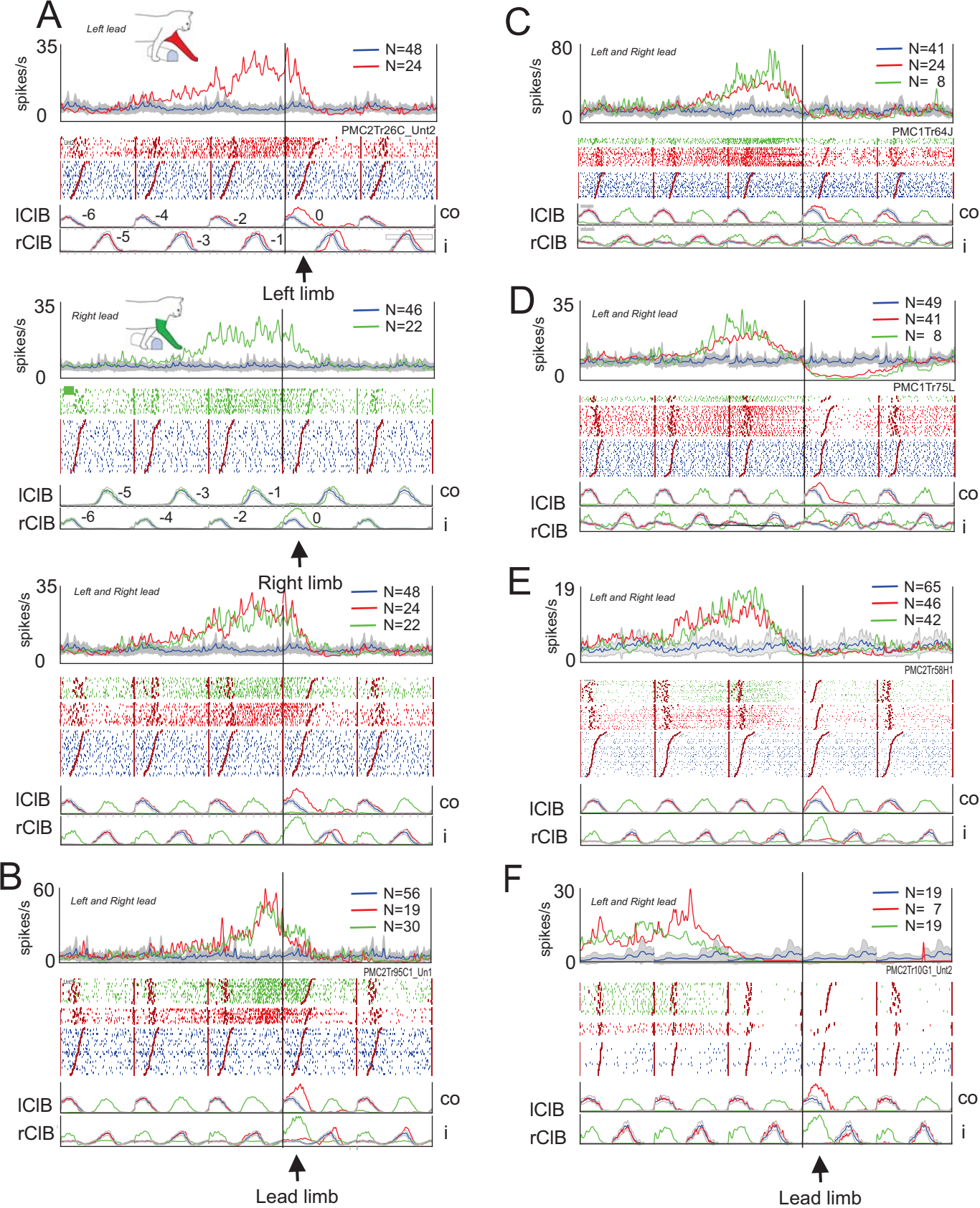
A
Left lead
35
0
spikes/s
N=48
N=24
PMC2Tr26C_Unt2
lCIB
rCIB
-6
-4
-2
0
-5
-3
-1
co
i
Left limb
Right lead
N=46
N=22
Right limb
Left and Right lead
N=48
N=24
N=22
B
60
N=56
N=19
N=30
PMC2Tr95C1_Un1
Lead limb
C
80
N=41
N=24
N= 8
PMC1Tr64J
D
N=49
N=41
N= 8
PMC1Tr75L
E
19
N=65
N=46
N=42
PMC2Tr58H1
F
30
N=19
N= 7
N=19
PMC2Tr10G1_Unt2

Fig. 5

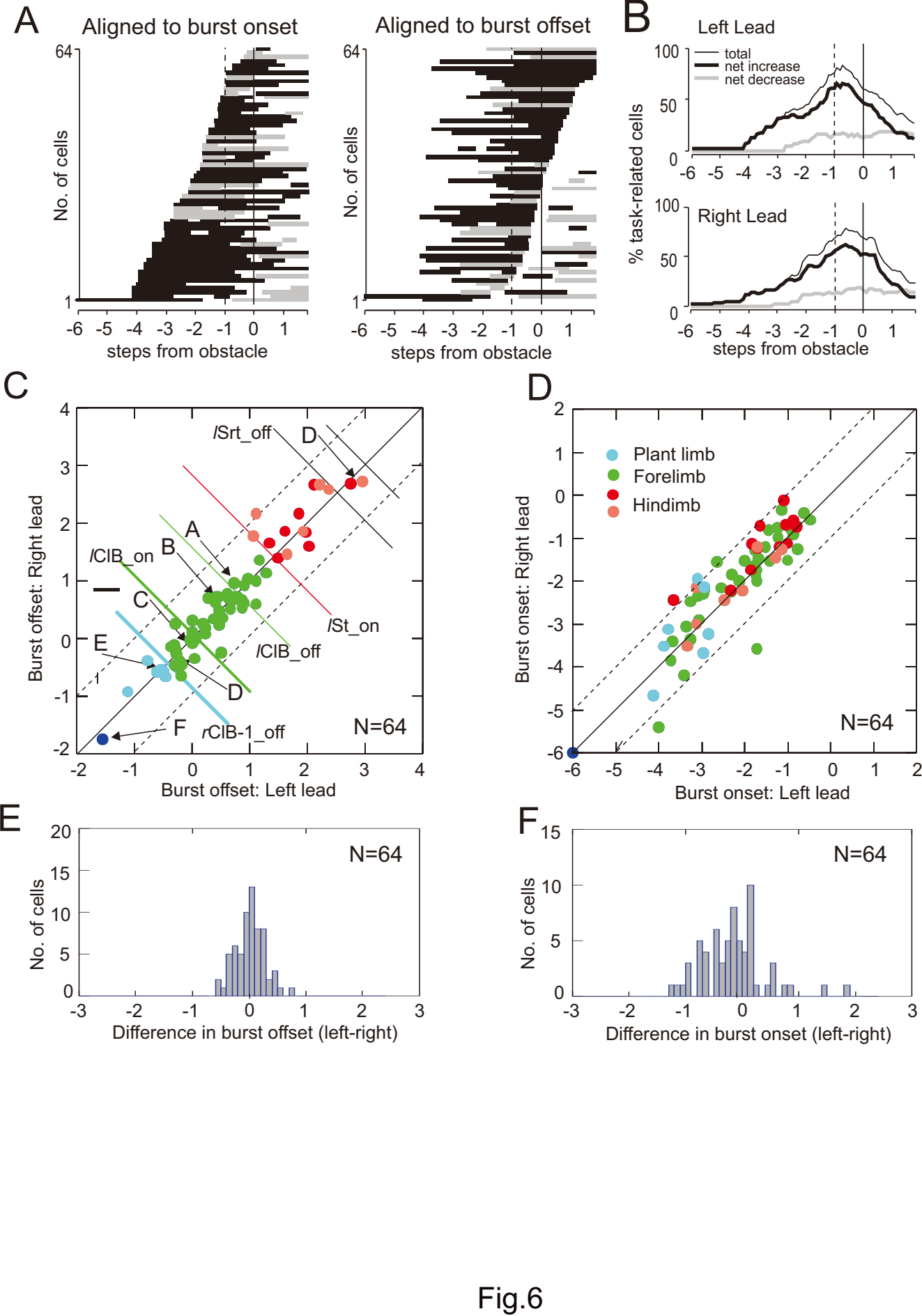
A
Aligned to burst onset
Aligned to burst offset
No. of cells
steps from obstacle
B
Left Lead
Right Lead
total
net increase
net decrease
% task-related cells
C
/Srt_off
/St_on
/ClB_on
/ClB_off
rClB-1_off
Burst offset: Right lead
Burst offset: Left lead
N=64
D
Plant limb
Forelimb
Hindimb
Burst onset: Right lead
Burst onset: Left lead
E
Difference in burst offset (left-right)
F
Difference in burst onset (left-right)

Fig.6

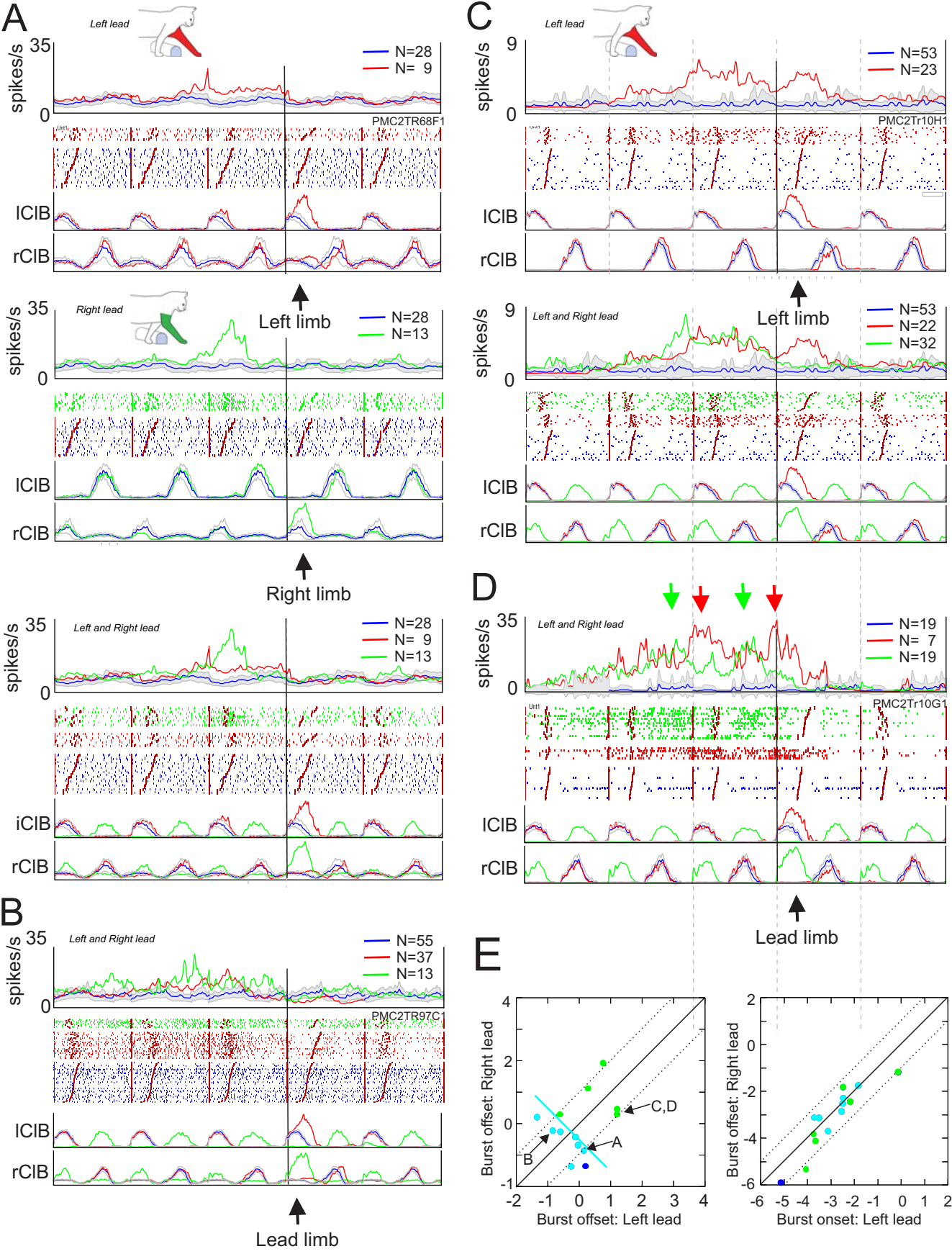
A
Left lead
spikes/s
35
0
N=28
N= 9
PMC2TR68F1
lCIB
rCIB
Right lead
Left limb
N=28
N=13
Right limb
Left and Right lead
N=28
N= 9
N=13
iCIB
B
N=55
N=37
N=13
PMC2TR97C1
Lead limb
C
N=53
N=23
PMC2Tr10H1
N=53
N=22
N=32
D
N=19
N= 7
N=19
PMC2Tr10G1
E
Burst offset: Right lead
Burst offset: Left lead
C,D
A
B
Burst onset: Left lead

Fig. 7

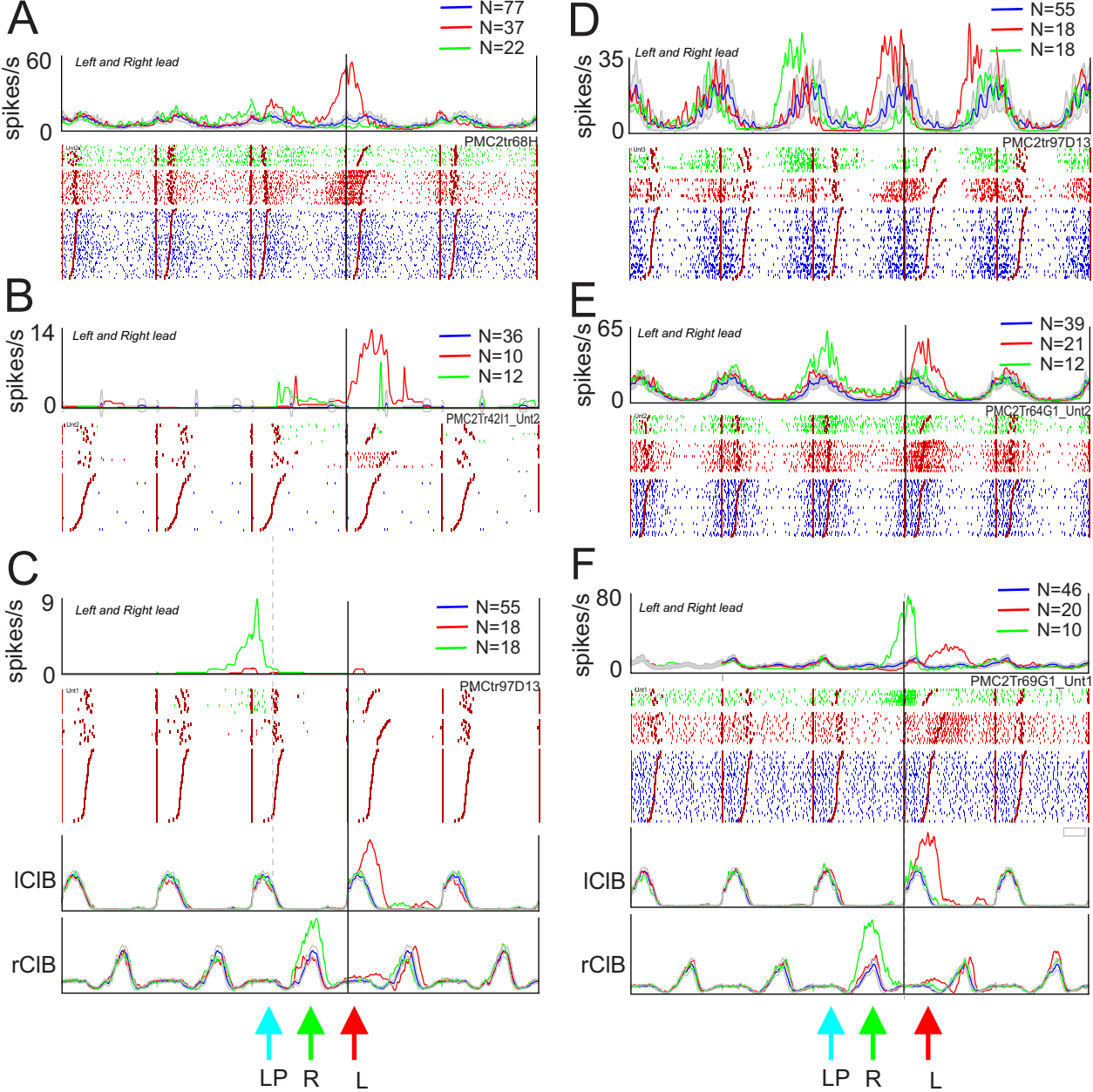
A
N=77
N=37
N=22
spikes/s
60
0
Left and Right lead
PMC2tr68H
B
14
0
Left and Right lead
N=36
N=10
N=12
PMC2Tr42I1_Unt2
C
9
0
Left and Right lead
N=55
N=18
N=18
PMCtr97D13
lClB
rClB
LP
R
L
D
N=55
N=18
N=18
35
0
Left and Right lead
PMC2tr97D13
E
65
0
Left and Right lead
N=39
N=21
N=12
PMC2Tr64G1_Unt2
F
80
0
Left and Right lead
N=46
N=20
N=10
PMC2Tr69G1_Unt1
lClB
rClB
LP
R
L

Fig. 8

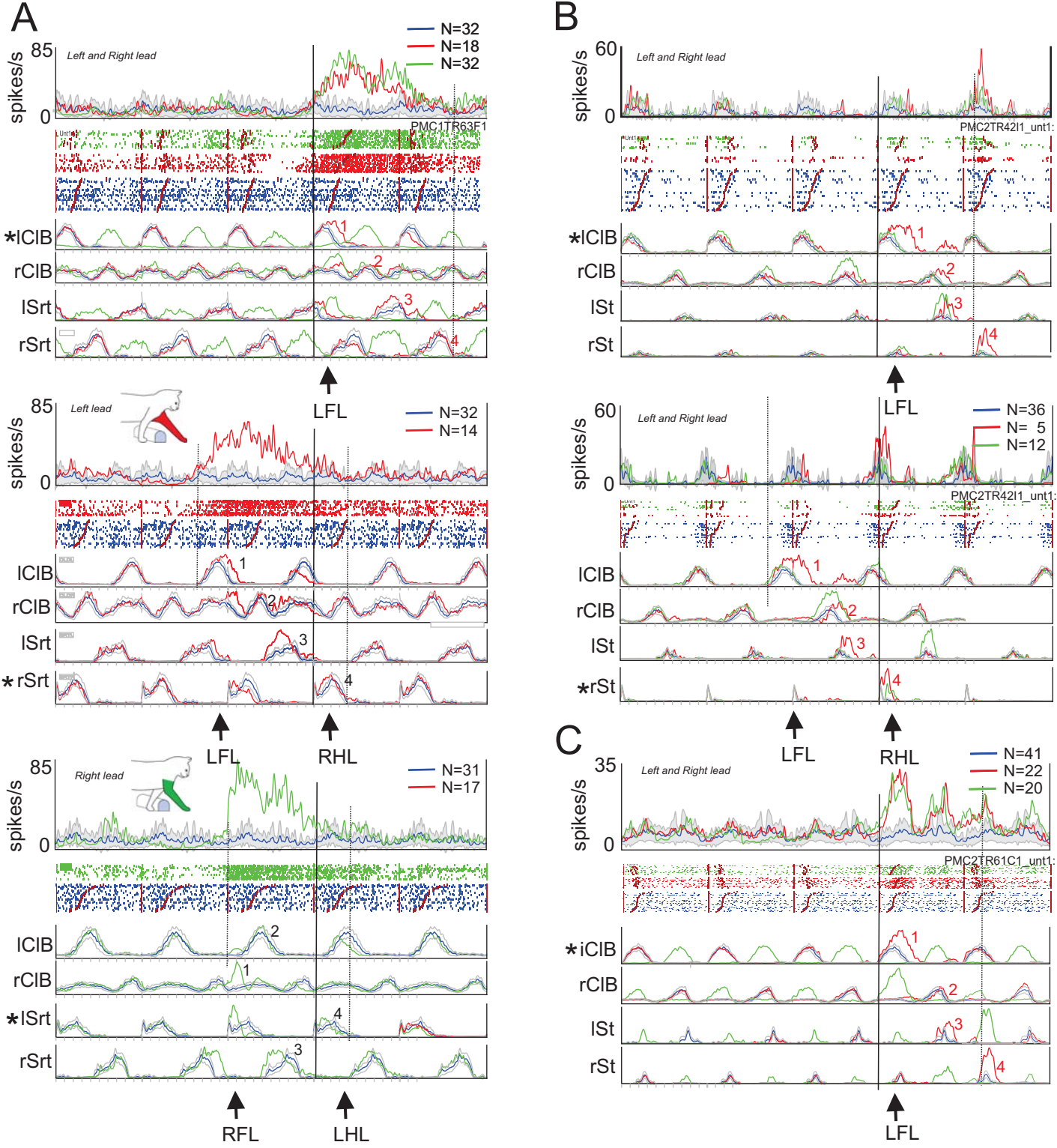
A
spikes/s
85
0
Left and Right lead
N=32
N=18
N=32
PMC1TR63F1
*lCIB
rCIB
lSrt
rSrt
1
2
3
4
LFL
Left lead
N=32
N=14
lCIB
rCIB
lSrt
*rSrt
LFL
RHL
Right lead
N=31
N=17
lCIB
rCIB
*lSrt
rSrt
RFL
LHL
B
spikes/s
60
0
Left and Right lead
PMC2TR42I1_unt1:
*lCIB
rCIB
lSt
rSt
LFL
Left and Right lead
N=36
N= 5
N=12
PMC2TR42I1_unt1:
lCIB
rCIB
lSt
*rSt
LFL
RHL
C
spikes/s
35
0
Left and Right lead
N=41
N=22
N=20
PMC2TR61C1_unt1:
*iCIB
rCIB
lSt
rSt
LFL

Fig. 9

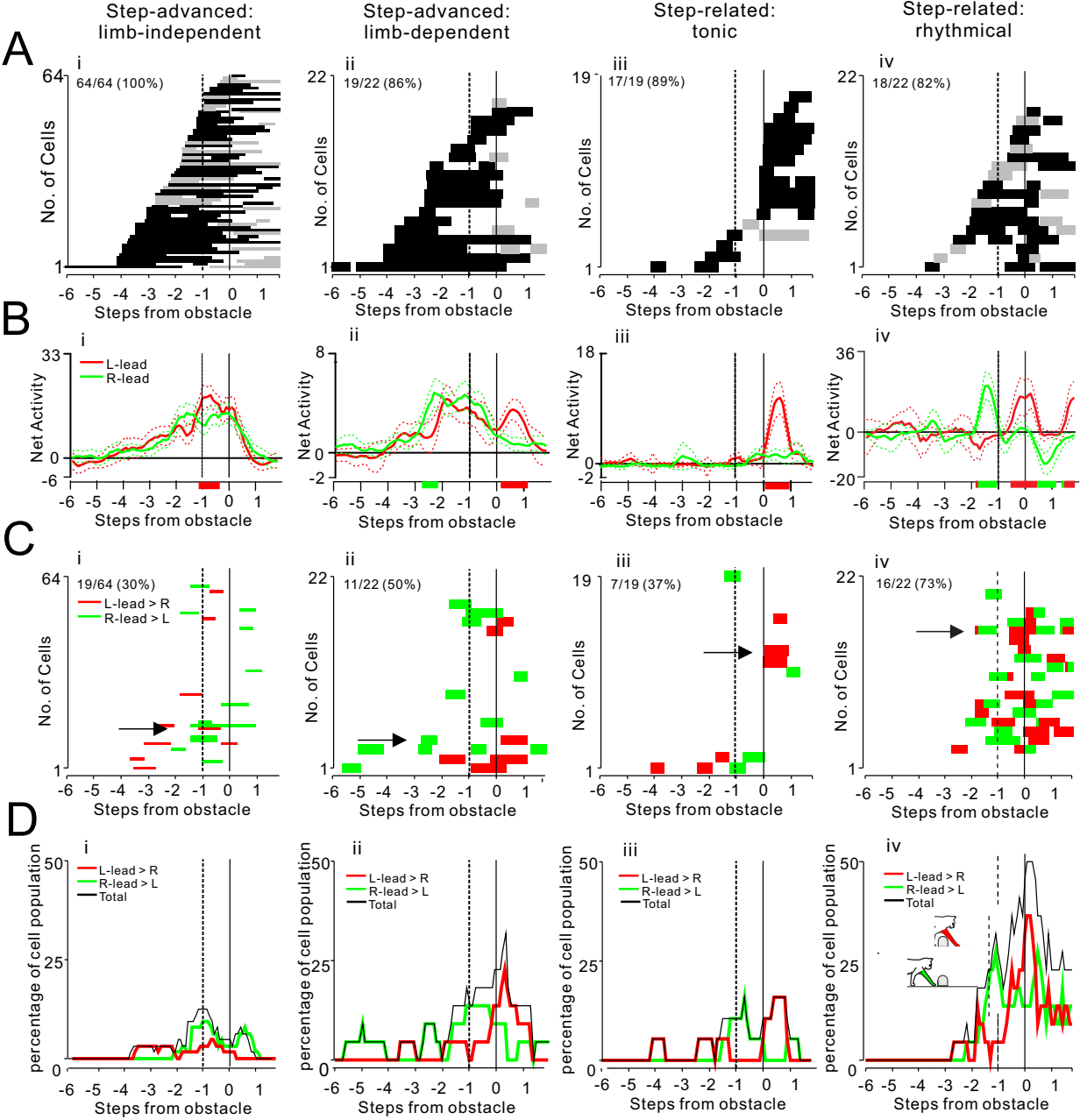
Step-advanced: limb-independent
Step-advanced: limb-dependent
Step-related: tonic
Step-related: rhythmical
A
B
C
D
i
ii
iii
iv
64/64 (100%)
19/22 (86%)
17/19 (89%)
18/22 (82%)
No. of Cells
Steps from obstacle
Net Activity
L-lead
R-lead
19/64 (30%)
11/22 (50%)
7/19 (37%)
16/22 (73%)
L-lead > R
R-lead > L
percentage of cell population
Total

Fig. 10

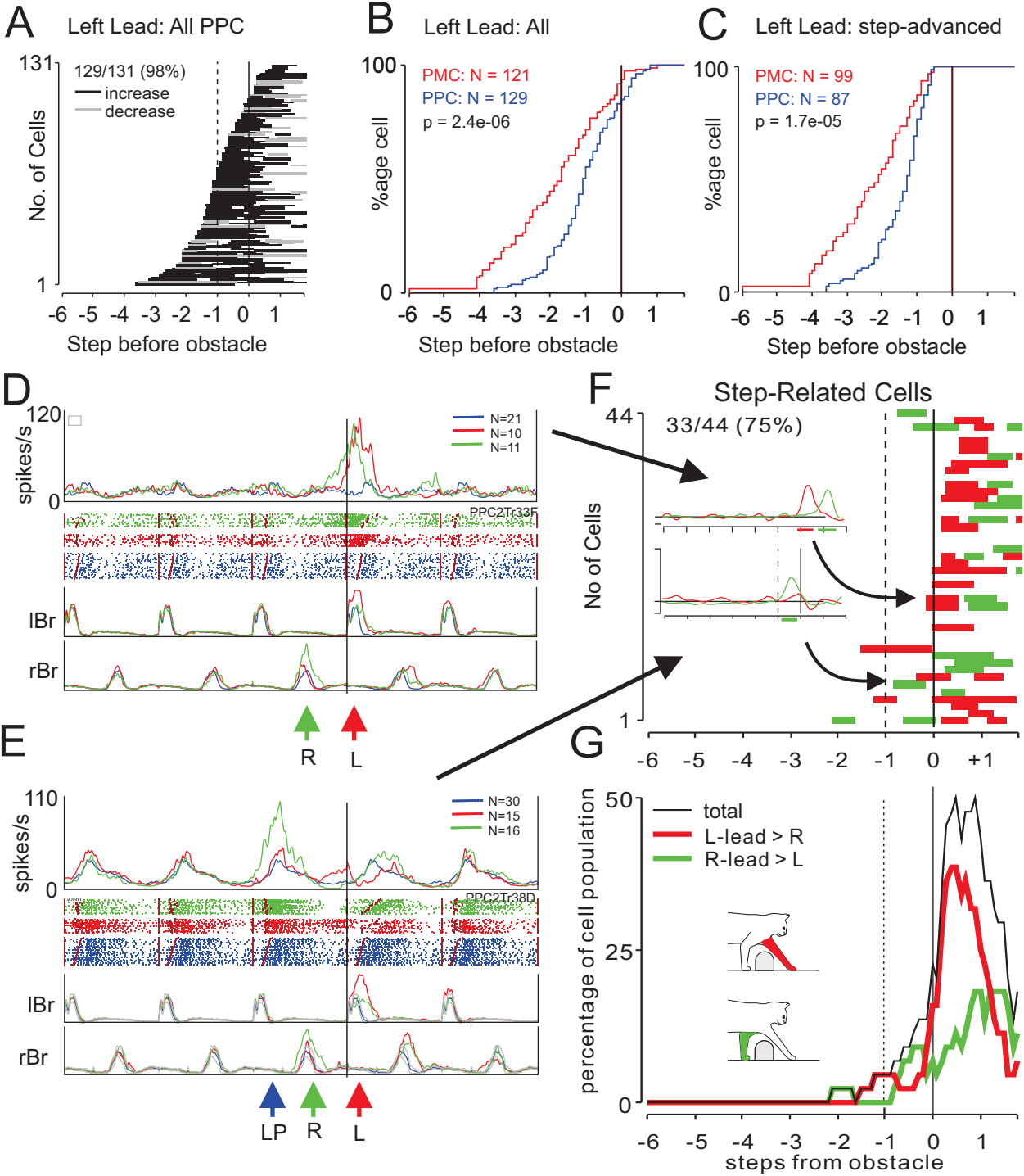
A
Left Lead: All PPC
131
129/131 (98%)
increase
decrease
No. of Cells
1
-6 -5 -4 -3 -2 -1 0 1
Step before obstacle
B
Left Lead: All
100
PMC: N = 121
PPC: N = 129
p = 2.4e-06
%age cell
0
-6 -5 -4 -3 -2 -1 0 1
Step before obstacle
C
Left Lead: step-advanced
100
PMC: N = 99
PPC: N = 87
p = 1.7e-05
%age cell
0
-6 -5 -4 -3 -2 -1 0 1
Step before obstacle
D
120
spikes/s
0
N=21
N=10
N=11
PPC2Tr33F
lBr
rBr
R
L
E
110
spikes/s
0
N=30
N=15
N=16
PPC2Tr38D
lBr
rBr
LP
R
L
F
Step-Related Cells
44
33/44 (75%)
No of Cells
1
-6 -5 -4 -3 -2 -1 0 +1
G
50
total
L-lead > R
R-lead > L
percentage of cell population
25
0
-6 -5 -4 -3 -2 -1 0 1
steps from obstacle

Fig. 11

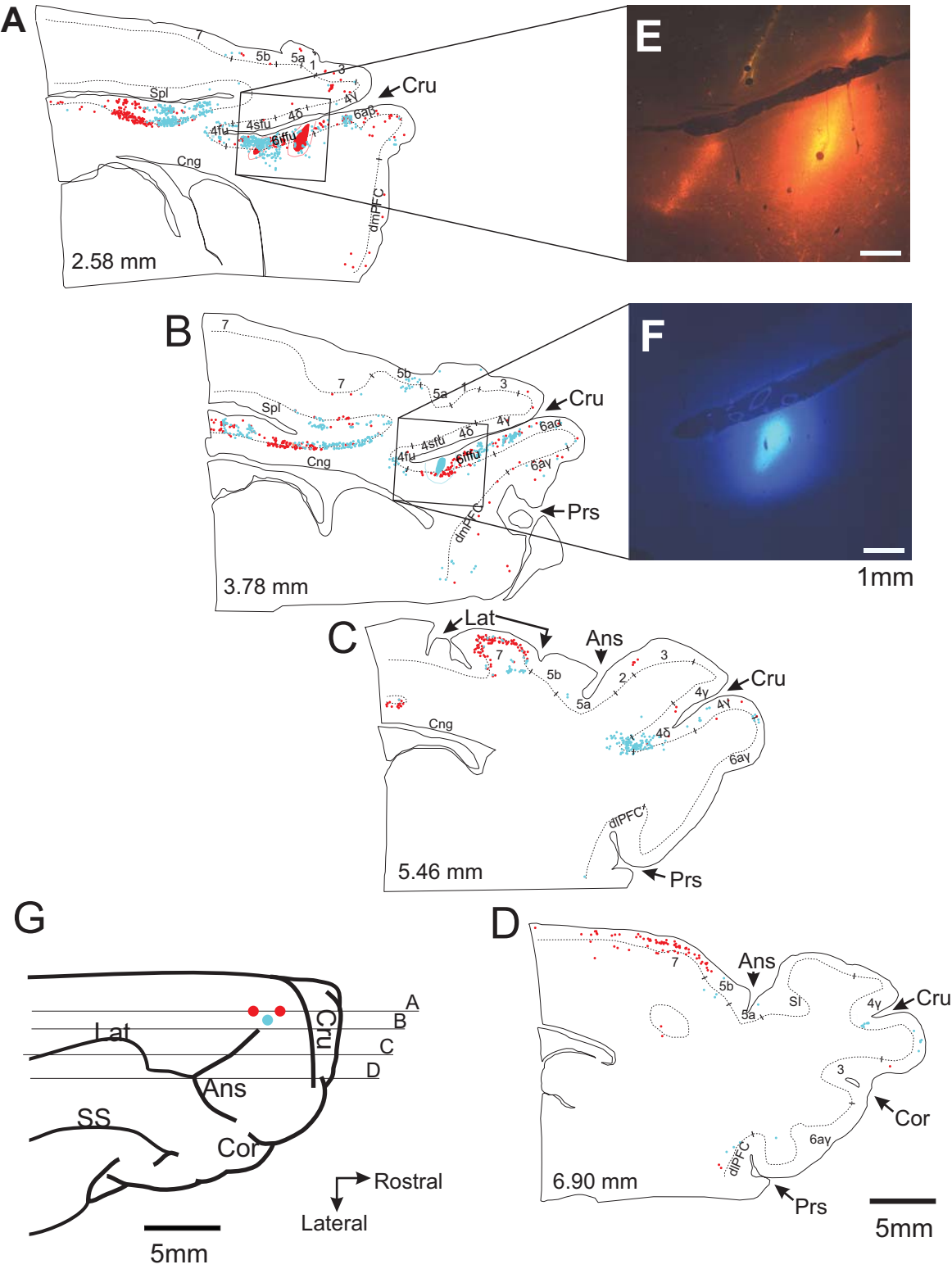
A
E
Cru
Spl
Cng
dmPFC
2.58 mm
B
F
Prs
3.78 mm
1mm
C
Lat
Ans
5.46 mm
G
D
Lat
Ans
SS
Cor
Rostral
Lateral
5mm
6.90 mm
5mm

Fig. 12

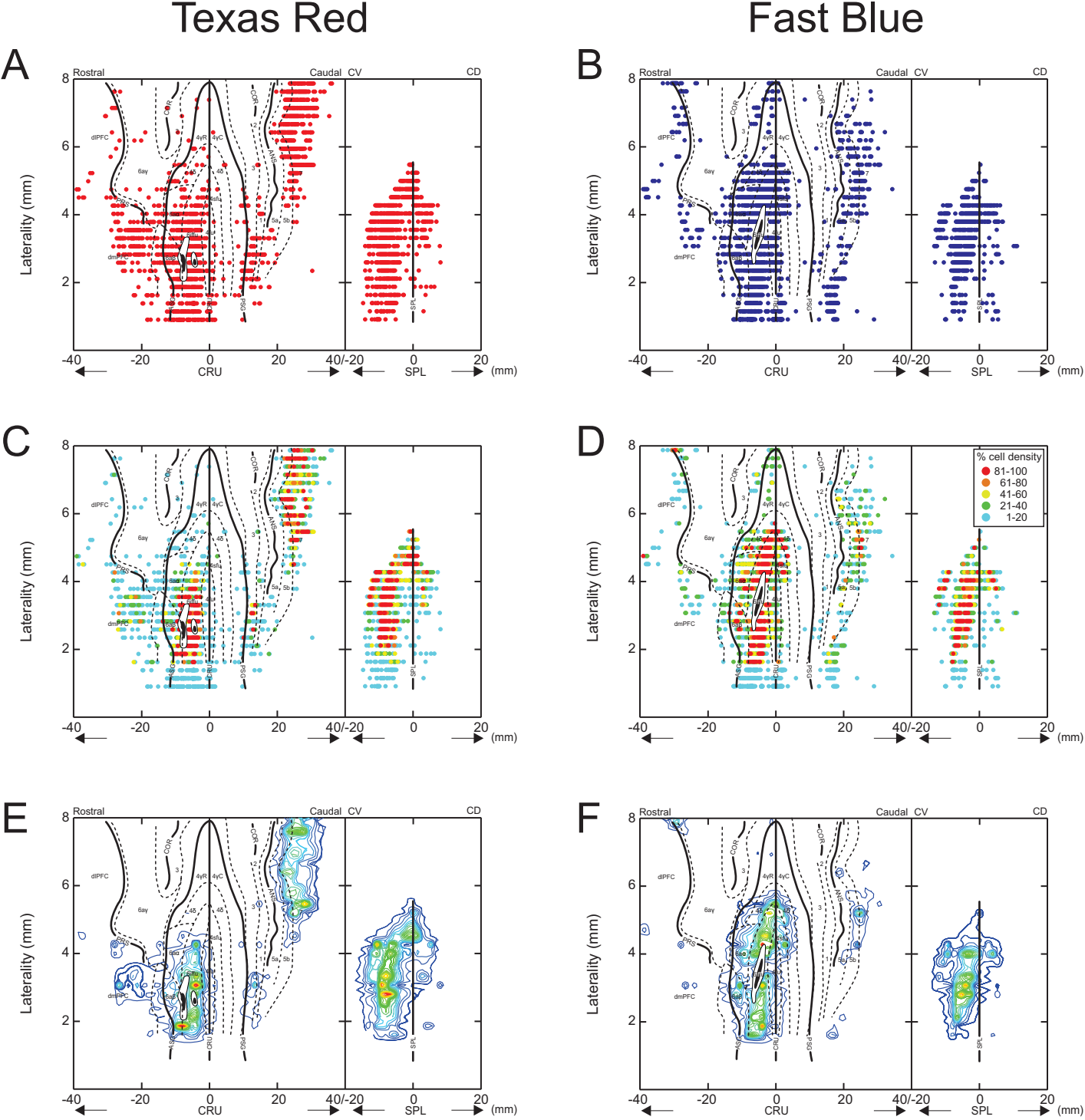
Texas Red
Fast Blue
A
B
C
D
E
F
Rostral
Caudal
CV
CD
Laterality (mm)
CRU
SPL
(mm)
% cell density
81-100
61-80
41-60
21-40
1-20

Fig. 13

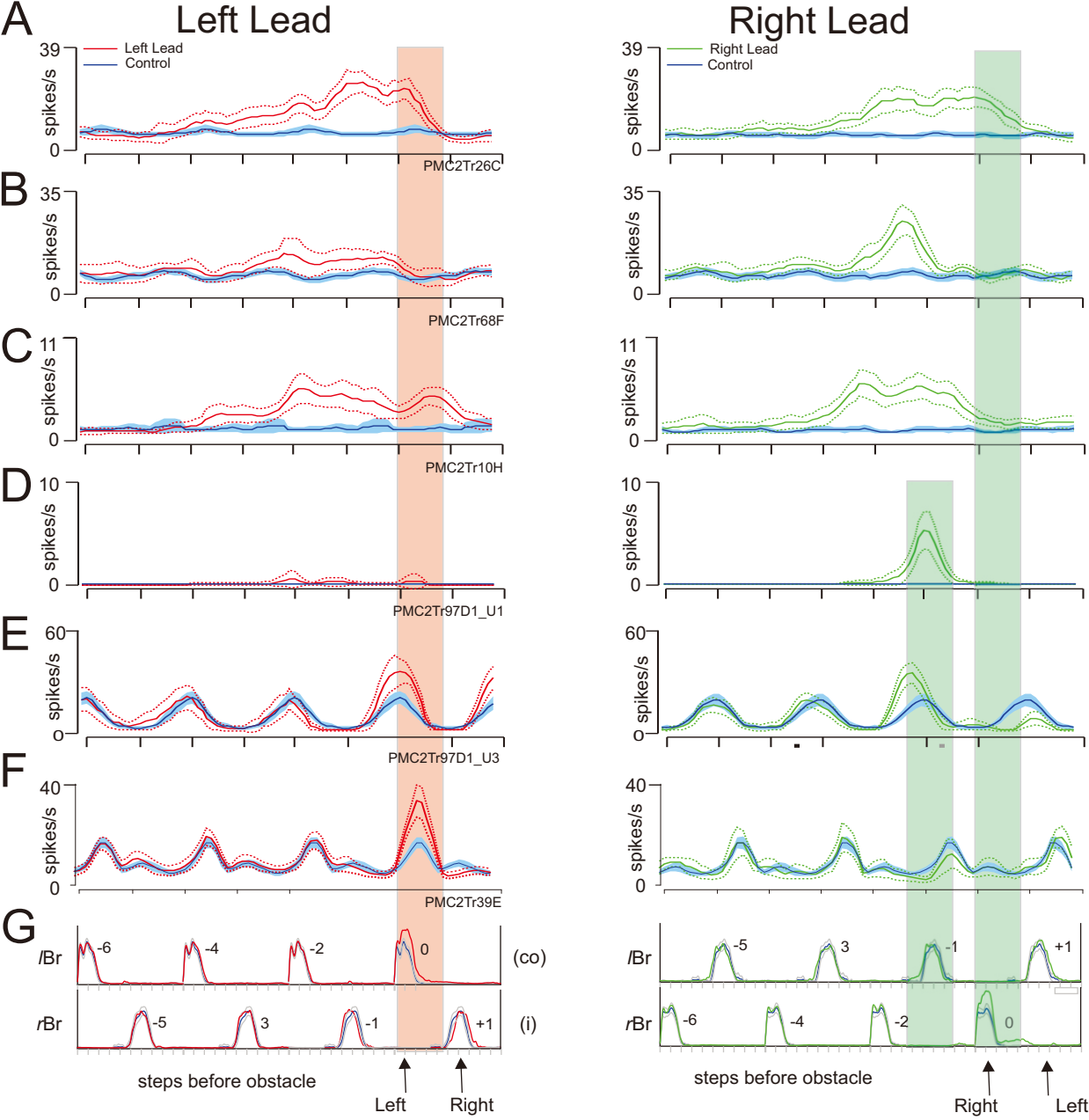
A
Left Lead
Right Lead
Left Lead
Control
Right Lead
Control
39
spikes/s
0
PMC2Tr26C
B
35
PMC2Tr68F
C
11
PMC2Tr10H
D
10
PMC2Tr97D1_U1
E
60
PMC2Tr97D1_U3
F
40
PMC2Tr39E
G
lBr
rBr
-6
-4
-2
0
(co)
-5
3
-1
+1
(i)
steps before obstacle
Left
Right

Fig. 14

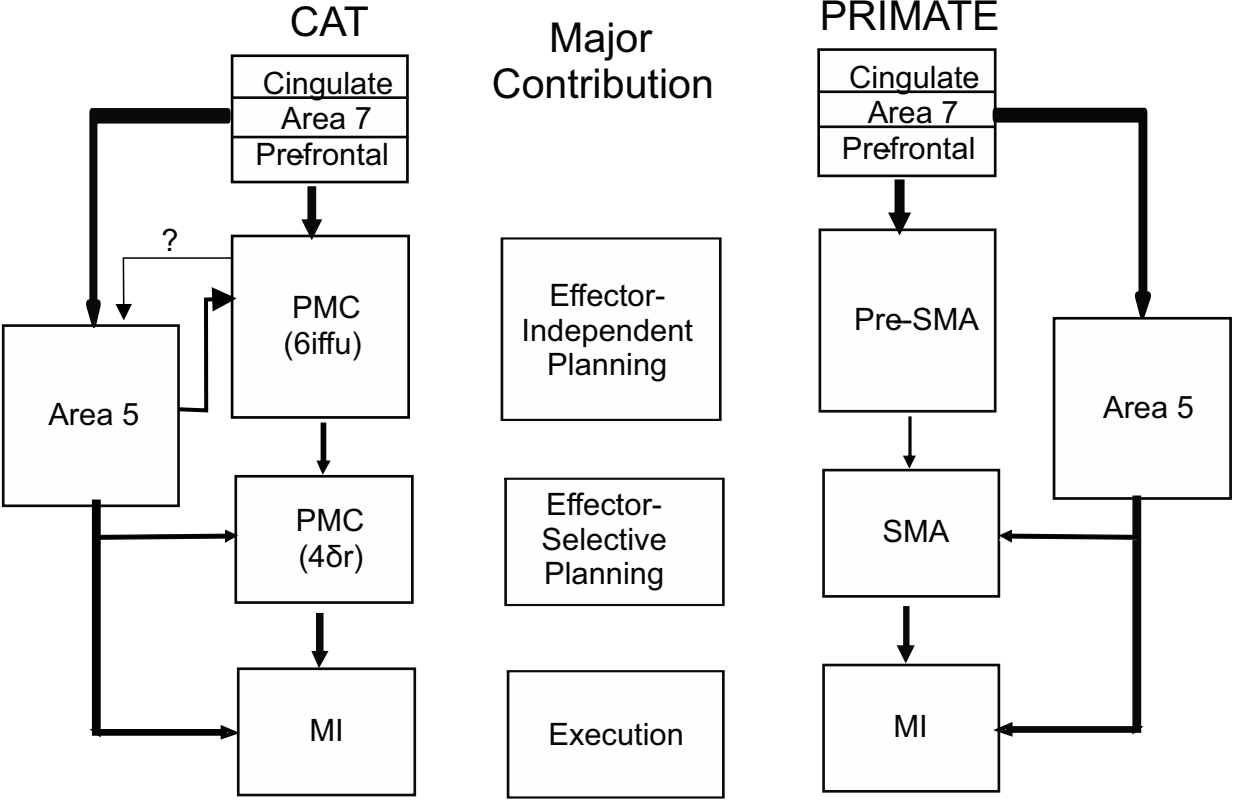
CAT
Major Contribution
PRIMATE
Cingulate
Area 7
Prefrontal
?
PMC (6iffu)
Area 5
PMC (4δr)
MI
Effector-Independent Planning
Effector-Selective Planning
Execution
Cingulate
Area 7
Prefrontal
Pre-SMA
SMA
MI
Area 5

Fig. 15

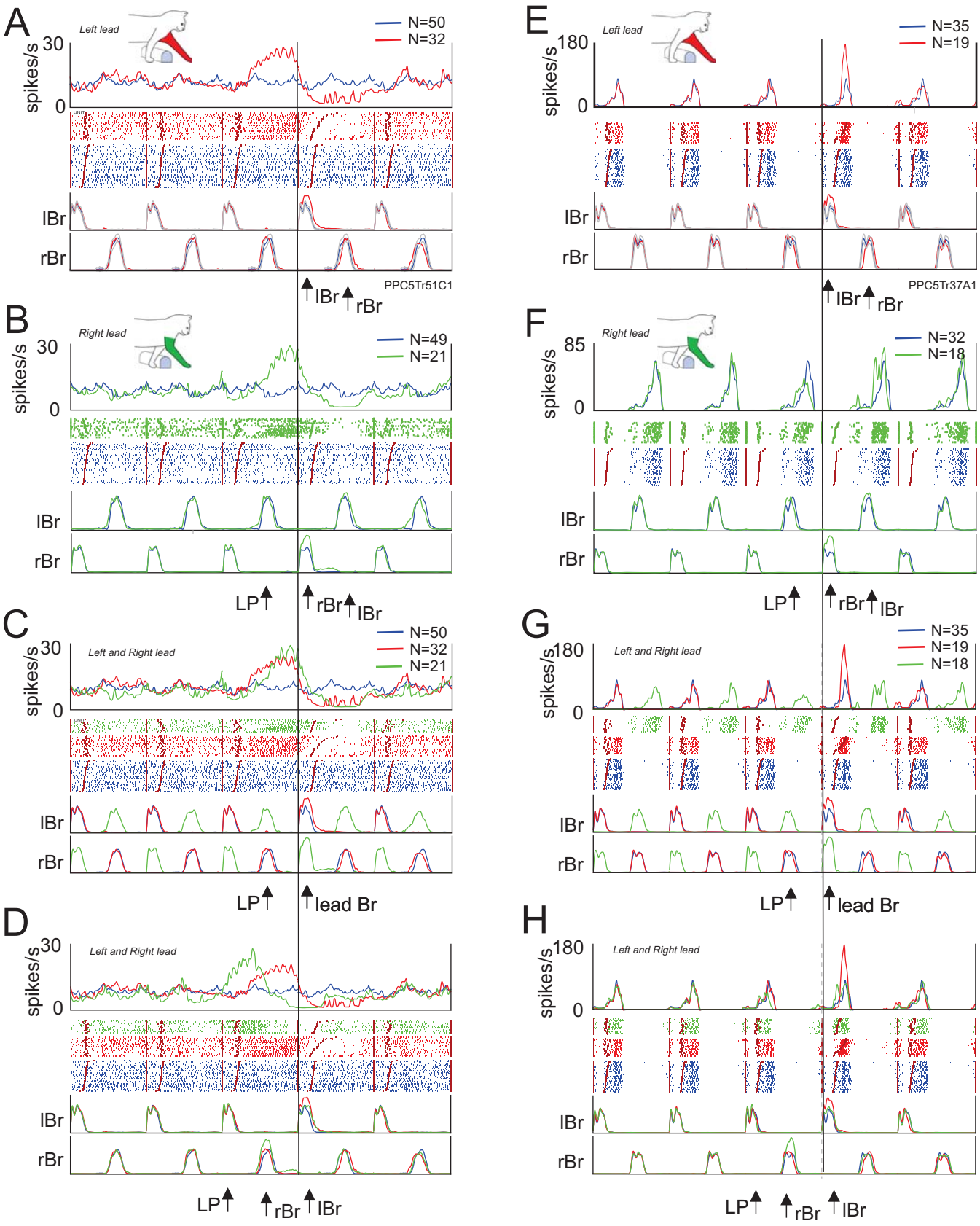
A
Left lead
N=50
N=32
spikes/s
30
0
lBr
rBr
PPC5Tr51C1
lBr
rBr
B
Right lead
N=49
N=21
spikes/s
30
0
lBr
rBr
LP
rBr
lBr
C
Left and Right lead
N=50
N=32
N=21
spikes/s
30
0
lBr
rBr
LP
lead Br
D
Left and Right lead
spikes/s
30
0
lBr
rBr
LP
rBr
lBr
E
Left lead
N=35
N=19
spikes/s
180
0
lBr
rBr
PPC5Tr37A1
lBr
rBr
F
Right lead
N=32
N=18
spikes/s
85
0
lBr
rBr
LP
rBr
lBr
G
Left and Right lead
N=35
N=19
N=18
spikes/s
180
0
lBr
rBr
LP
lead Br
H
Left and Right lead
spikes/s
180
0
lBr
rBr
LP
rBr
lBr

Fig. S1

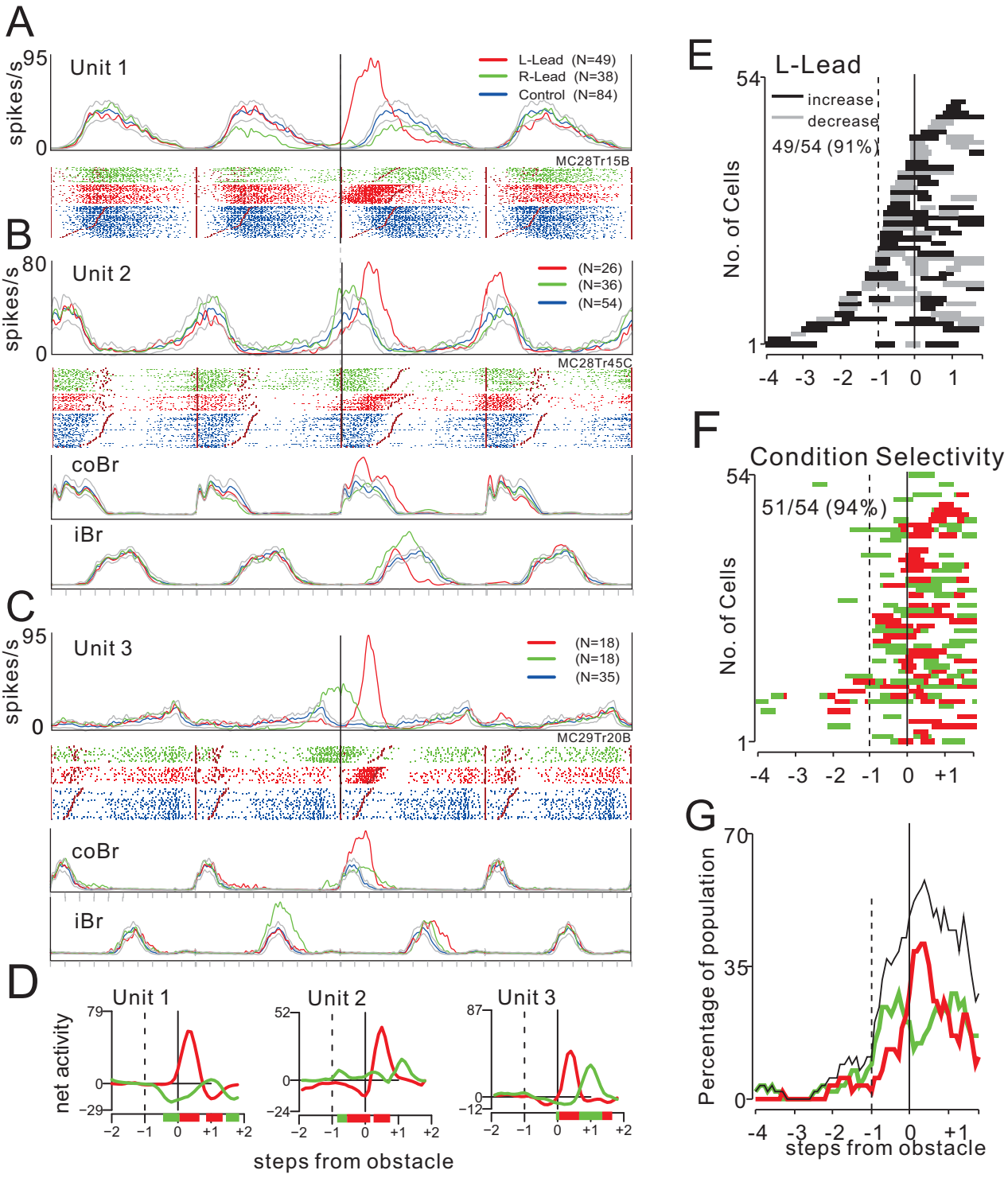
A
Unit 1
spikes/s
95
0
L-Lead (N=49)
R-Lead (N=38)
Control (N=84)
MC28Tr15B
B
Unit 2
spikes/s
80
0
(N=26)
(N=36)
(N=54)
MC28Tr45C
coBr
iBr
C
Unit 3
spikes/s
95
0
(N=18)
(N=18)
(N=35)
MC29Tr20B
coBr
iBr
D
Unit 1
Unit 2
Unit 3
net activity
79
0
-29
52
0
-24
87
0
-12
−2 −1 0 +1 +2
steps from obstacle
E
L-Lead
54
1
increase
decrease
49/54 (91%)
No. of Cells
-4 -3 -2 -1 0 1
F
Condition Selectivity
54
1
51/54 (94%)
No. of Cells
-4 -3 -2 -1 0 +1
G
70
35
0
Percentage of population
-4 -3 -2 -1 0 +1
steps from obstacle

Fig. S2